UC San Diego

UC San Diego Electronic Theses and Dissertations

Title

Androgen Receptor in Kisspeptin Cells is Necessary for Reproductive Phenotypes following Prenatal Anti-Mullerian Hormone Exposure

Permalink

https://escholarship.org/uc/item/0c04h2m4

Author

Ho, Emily Volena

Publication Date

2021

Peer reviewed|Thesis/dissertation

UNIVERSITY OF CALIFORNIA SAN DIEGO

Androgen Receptor in Kisspeptin Cells is Necessary for Reproductive Phenotypes following
Prenatal Anti-Mullerian Hormone Exposure

A dissertation submitted in partial satisfaction of the requirements for the degree Doctor of
Philosophy

in

Neurosciences

by

Emily Volena Ho

Committee in Charge:

      Professor Pamela Mellon, Chair
      Professor Kellie Breen Church
      Professor Heidi Cook-Andersen
      Professor Alexander Kauffman
      Professor Varykina Thackray

2021

The dissertation of Emily Volena Ho is approved, and it is acceptable in quality and form for publication on microfilm and electronically.

University of California San Diego

2021

DEDICATION

To my parents—Brenda Anne Wilson and Mengfei Ho—and my brother, Brian Ho.

May the critical thought and dogged perseverance that I poured into this work

fill them with pride.

EPIGRAPH

Few men can keep alive through a big surf
to crawl, clotted with brine, on kindly beaches
in joy, in joy, knowing the abyss behind.

Homer, *Odyssey*

TABLE OF CONTENTS

LIST OF ABBREVIATIONS

AMH	Anti-Mullerian hormone
AMHR2	Anti-Mullerian hormone receptor type-2
AR	Androgen receptor
E_2	Estradiol
F_1	First generation
F_2	Second generation
FSH	Follicle-stimulating hormone
GnRH	Gonadotropin-releasing hormone
GWAS	Genome-wide association study
HPG	Hypothalamic-pituitary-gonadal
KARKO	Kisspeptin-specific androgen receptor knockout
LH	Luteinizing hormone
P	Postnatal day
P_4	Progesterone
pAMH	Prenatal anti-Mullerian hormone
PCOS	Polycystic ovary syndrome
T	Testosterone
tdT	tdTomato

LIST OF FIGURES

LIST OF TABLES

LIST OF SCHEMAS

ACKNOWLEDGEMENTS

I would first like to thank my wonderful advisor Dr. Pamela Mellon, for taking me on and welcoming me into exactly the lab environment I needed to survive and thrive during my PhD training. My grad school experience has been enriched by exceptional people. I am especially grateful for my lab mates Karen Tonsfeldt, Jessica Cassin, Shanna Newton Lavalle, and Erica Pandolfi who have all supported me in countless ways, ranging from technical training to big picture brainstorming to heartwarming friendship. I would also like to thank Victoria (Chengxian) Shi and the rest of Team AMH for their assistance with experiments and for allowing me to witness their growth as mentees and people over the years we have worked together.

I also thank my thesis committee members—Alexander (Sasha) Kauffman, Kellie Breen Church, Varykina (Kina) Thackray, and Heidi Cook-Andersen—for their time, interest, and guidance as I have navigated this project. I would also like to acknowledge the Medical Scientist Training Program, the Neurosciences Graduate Program, and the Genetics Training Program. Being part of these communities—having on faculty, administrators, and peers to lean on—has been instrumental in my success.

Finally, I would like to thank my family and dear friends for their love, which has carried me through every moment my PhD—big and small, light and heavy, exciting and mundane. I would not be where I am today without my husband Kevin Psolka-Green—my partner, my rock, my warmth. I am endlessly grateful for being able to come home to him and our furry family.

All chapters of this dissertation have been submitted for publication in *eLife* (**Ho, Emily V.**; Shi, Chengxian; Cassin, Jessica; He, Michelle Y.; Nguyen, Ryan D.; Ryan, Genevieve E.; Mellon, Pamela L. Androgen Receptor in Kisspeptin Cells is Necessary for Reproductive

Phenotypes following Prenatal Anti-Mullerian Hormone Exposure. *eLife*. 2021. [Submitted]).

The dissertation author was the primary investigator and author of this paper. Chengxian Shi assisted with execution of experiments. Jessica Cassin provided guidance on experimental design and manuscript composition, as well as critical troubleshooting. Michelle He and Ryan Nyugen assisted with data collection. Genevieve Ryan generated the cell-specific mouse line. Karen Tonsfeldt contributed immunohistochemistry and imaging, as well as assistance with manuscript composition. Pamela Mellon supervised the project and provided advice.

2013   Bachelor of the Arts, Biological Sciences and Psychology, University of Chicago

2021   Doctor of Philosophy, Neurosciences, University of California San Diego

PUBLICATIONS

Ho, Emily V.; Shi, Chengxian; Cassin, Jessica; He, Michelle Y.; Nguyen, Ryan D.; Ryan, Genevieve E.; Mellon, Pamela L. Androgen Receptor in Kisspeptin Cells is Necessary for Reproductive Phenotypes following Prenatal Anti-Mullerian Hormone Exposure. *eLife*. 2021. [Submitted].

Ryan, Genevieve E.; Bohaczuk, Stephanie C.; Cassin, Jessica; Witham, Emily A.; Shojaei, Shadi; **Ho, Emily V.**; Thackray, Varykina G.; Mellon, Pamela L. Androgen Receptor Positively Regulates Gonadotropin-releasing Hormone Receptor in Pituitary Gonadotropes. *Molecular and Cellular Endocrinology*. 2021 Apr 16;111286. doi: 10.1016/j.mce.2021.111286.

Thompson, Summer L.; Welch, Amanda; **Ho, Emily V.**; Bessa, Joao; Portugal-Nunes, Carlos; Morais, Monica; Young, Jared; Knowles, James A.; Dulawa, Stephanie C. Hippocampal Btbd3 expression regulates compulsive-like behavior. *Translational Psychiatry*. 2019 Sep 9;9(1):222. doi: 10.1038/s41398-019-0558-7.

Pospos, Sarah; Tal, Ilanit; Iglewicz, Alana; Newton, Isabelle G.; Tai-Seale, Ming; Downs, Nancy; Jong, Pamela M.; Lee, Daniel; Davidson, Judy E.; Lee, Soo Y.; Rubanovich, Caryn K.; **Ho, Emily V.;** Sanchez, Courtney; Zisook, Sidney. Gender Differences among Medical Students, House Staff and Faculty Physicians at High Risk for Suicide: A HEAR Report. *Depression & Anxiety*. 2019 Oct;36(10):902-920. doi: 10.1002/da.22909. Epub 2019 May 17.

Coba, Marcelo P.; Ramaker, Marcia J.; **Ho, Emily V.**; Thompson, Summer L.; Komiyama, Noboru H.; Grant, Seth G.N.; Knowles, James A.; Dulawa, Stephanie C. DLGAP1 knockout mice exhibit alterations of the postsynaptic density and selective impairments in social interaction. *Scientific Reports*. 2018 Feb 2;8(1):2281. doi: 10.1038/s41598-018-20610-y.

Lev-Ari, Shiri, **Ho, Emily V.**; Keysar, Boaz. The unforeseen consequences of interacting with non-native speakers. *Topics in Cognitive Science.* 2018 Oct;10(4):835-849. doi: 10.1111/tops.12325. Epub 2018 Feb 7.

Ho, Emily V.; Klenotich, Stephanie J.; McMurray, Matthew S.; Dulawa, Stephanie C. Activity-Based Anorexia Alters the Expression of BDNF Transcripts in the Mesocorticolimbic

Reward Circuit. *PLoS ONE*. 2016 Nov 18;11(11):e0166756. doi: 10.1371/journal.pone.0166756. eCollection 2016.

Ho, Emily V.; Thompson, Summer L.; Katzka, William R.; Sharifi, Mitra S.; Knowles, James A.; Dulawa, Stephanie C. Clinically effective OCD treatment prevents 5-HT1B receptor-induced behaviors and striatal activation. *Psychopharmacology*. 2016 Jan;233(1):57-70. doi: 10.1007/s00213-015-4086-8. Epub 2015 Sep 30.

Klenotich, Stephanie J.; **Ho, Emily V.**; Server, Christine H.; McMurray, Matthew S.; Dulawa, Stephanie C. Subchronic antagonism of dopamine D2/3 receptors is sufficient to increase survival in activity-based anorexia in mice. *Translational Psychiatry*. 2015 Aug 4;5(8):e613. doi: 10.1038/tp.2015.109.

Woehrle, Nancy S.; Klenotich, Stephanie J.; Jamnia, Naseem; **Ho, Emily V.**; Dulawa, Stephanie C. Effects of chronic fluoxetine treatment on serotonin 1B receptor-induced deficits in delayed alternation. *Psychopharmacology*. 2013 Jun;227(3):545-51. Epub 2013 Feb 3.

ABSTRACT OF THE DISSERTATION

Androgen Receptor in Kisspeptin Cells is Necessary for Reproductive Phenotypes following
Prenatal Anti-Mullerian Hormone Exposure

by

Emily Volena Ho

Doctor of Philosophy in Neurosciences

University of California San Diego, 2021

Professor Pamela Mellon, Chair

Polycystic ovary syndrome (PCOS) is a common reproductive disorder characterized by elevated androgens and anti-Mullerian hormone (AMH). These hormones remain elevated throughout pregnancy, and potential effects of hormone exposure on offspring from women with PCOS remain largely unexplored. Expanding on recent reports of prenatal AMH exposure in mice, we have fully characterized the reproductive consequences of prenatal AMH (pAMH)

exposure throughout the lifespan of first- and second-generation offspring of both sexes. We also sought to elucidate mechanisms underlying pAMH-induced reproductive effects. There is a known reciprocal relationship between AMH and androgens, and in PCOS and PCOS-like animal models, androgen feedback is dysregulated at the level the hypothalamus. Kisspeptin neurons express androgen receptors and play a critical role in sexual development and function. We therefore hypothesized that pAMH-induced reproductive phenotypes would be mediated by androgen signaling at the level of kisspeptin cells. We tested the pAMH model in kisspeptin-specific androgen receptor knockout (KARKO) mice and found that virtually all pAMH-induced phenotypes assayed are eliminated in KARKO offspring compared to littermate controls. By demonstrating the necessity of androgen receptor in kisspeptin cells to induce pAMH phenotypes, we have advanced understanding of the interactions between AMH and androgens in the context of prenatal exposure, which could have significant implications for children of women with PCOS.

INTRODUCTION

Polycystic Ovary Syndrome (PCOS)

Polycystic ovary syndrome (PCOS) affects 1 in 10 reproductive-age women and is the most common cause of anovulatory infertility (1). PCOS classically presents with disrupted ovulation in the form of irregular menstrual cycles and failure to conceive, polycystic ovaries on ultrasound due to an increase in unruptured, immature follicles, and androgen excess that results in hirsutism and acne. Elevated androgen levels in PCOS patients begins around puberty and extends into the ninth decade of life (2). Clinical studies suggest that androgens may be not only a diagnostic feature, but also play a causal role in the disorder (3-6).

Hyperandrogenism also persists throughout any pregnancies (7-10), with potential consequences for offspring. Daughters from women with PCOS have a 5-fold increased risk for developing PCOS themselves (11), and sons have been shown to have altered hormones during puberty (12, 13). Since loci identified by PCOS genome-wide association studies account for less than 10 percent of disease heritability (14) and over 20 percent of the variation observed in PCOS can be explained by environmental factors (15), non-genetic influences such as altered gestational hormones could confer risk to offspring.

The hypothalamic-pituitary-gonadal (HPG) axis

Androgens are a group of steroid hormones that include testosterone and androstenedione and mediate many physiological functions in both males and females by binding to androgen receptors (AR). Androgens are regulated by the reproductive neuroendocrine, or hypothalamic-pituitary-gonadal (HPG), axis (16). Pulsatile release of gonadotropin-releasing hormone (GnRH) from hypothalamic GnRH neurons stimulates gonadotropes in the anterior pituitary to release the gonadotropins luteinizing hormone (LH) and follicle-stimulating hormone (FSH). These

1

gonadotropins act on the gonads to regulate sex steroid hormones, such as androgens, estrogens, and progestins. Specifically, in females, LH binds to LH receptors in ovarian theca cells to increase synthesis of androgens, which can then be converted to estrogens by aromatase in granulosa cells and other tissues (17), and FSH binds to FSH receptors on ovarian granulosa cells to help support folliculogenesis and ovulation (18). In males, LH binds to receptors in testicular Leydig cells in the interstitial space to stimulate androgen production, and FSH binds to receptors in Sertoli cells present in the seminiferous tubules to generate regulator factors and nutrients needed for spermatogenesis (19). Sex steroid hormones also feedback to neuronal populations of the hypothalamus and pituitary gonadotropes to modulate their own release and exert neuroendocrine function.

Because GnRH neurons themselves do not express AR, androgens likely act on an upstream, afferent neuronal population, possibly on hypothalamic kisspeptin neurons. Kisspeptin neurons in the arcuate nucleus (ARC) of the hypothalamus are considered the pacemakers of pulsatile GnRH release (20) and are critical for normal sexual maturation and function (21). ARC kisspeptin neurons do express AR, and androgenic signaling in the ARC results in decreased kisspeptin expression and suppression of LH pulses (22).

In PCOS and PCOS-like mouse models, sex steroid feedback to the HPG axis is altered. Despite the characteristic elevations in androgens, LH levels and pulsatility remain high (23-25). This is also evident by increased GnRH neuron excitability and pulsatile release of GnRH onto pituitary gonadotropes, favoring LH production and release over FSH and contributing to an increased LH:FSH ratio in PCOS patients (26).

Anti-Mullerian Hormone (AMH) and its alteration in PCOS

First isolated and purified in 1984, anti-Mullerian hormone (AMH) plays an important role in sexual differentiation and gonadal function (27). In males, developmental AMH produced by testicular Sertoli cells induces the regression of the Müllerian ducts then decreases markedly by puberty. In females, AMH production in developing ovarian follicles begins around birth and continues until menopause. Intraovarian AMH prevents excessive or premature recruitment and maturation of follicles (28). AMH is produced by granulosa cells in increasing amounts as the follicle develops from the preantral stages to the small antral stage. Once the follicle reaches the large antral stage, AMH becomes downregulated, allowing maturation to continue toward ovulation. In rodents, AMH has been shown to directly affect the HPG axis by binding to AMH receptor type II (AMHR2) on GnRH neurons, increasing their excitability and pulse-firing rate (29).

In addition to the characteristic increase in androgens, anti-Mullerian hormone (AMH) levels have been found to correlate with the severity of clinical manifestations of PCOS, including signs of hyperandrogenism (30-33), and genetic studies in PCOS women have identified associations between androgen levels and polymorphisms in the genes encoding AMH and its ligand-binding receptor, AMHR2 (34-36). In PCOS patients, ovarian follicles are arrested at a stage in follicular development when AMH production is highest (37), and each individual follicle produces more AMH than follicles from healthy controls (38). AMH levels in follicular fluid and serum are at least 5- and 3-fold higher, respectively, in PCOS women (39-41). These increased AMH levels remain elevated into the second trimester of pregnancy and at term (25, 42). The effects of prenatal AMH exposure on offspring have yet to be fully examined.

Prenatal AMH (pAMH) exposure

Although AMH is clearly dysregulated with PCOS, only one group has explored the effects of prenatal AMH (pAMH) exposure thus far (25, 43). In mice, peripheral administration of AMH late in gestation resulted in marked reproductive disruptions in female offspring (25). pAMH females showed delayed puberty and disrupted early estrous cycling, as well as alteration at all levels of the HPG axis. pAMH-induced reproductive phenotypes are transgenerational, with second and third generation females also affected (43). However, initial investigations did not examine timepoints beyond puberty and early adulthood. Assessments of late adulthood are especially relevant as *in utero* androgen exposure results in altered reproductive senescence in mice (44). Further, possible consequences to pAMH male offspring have not been explored and underlying pathophysiological mechanisms have yet to be fully elucidated.

One proposed pathway for pAMH to induce reproductive effects is AMH action at the level of the hypothalamus to activate the HPG axis and favor excess androgen production (25). Although peripherally administered AMH does not cross the placenta, it does alter maternal serum hormones and placental gene expression to create an androgenic environment *in utero* (25). Prenatal androgen excess in mice contributes to the development of PCOS-like reproductive features (44-47). pAMH phenotypes can be reversed and prevented with a GnRH antagonist (25), further suggesting a central, androgen-mediated mechanism. However, contribution of androgens to pAMH-induced phenotypes has not been directly tested.

Given androgen feedback dysregulation in PCOS, the role that ARC kisspeptin neurons play in sexual development and function, and known presence and function of AR in these cells, we hypothesized that the pAMH-induced reproductive phenotype would be mediated by androgen signaling at the level of kisspeptin cells.

4

Here, we characterize a full profile throughout the lifespan of first and second generation pAMH offspring of both sexes. Utilizing Cre-LoxP technology, we generated a kisspeptin-specific AR knockout (KARKO) mouse line and assessed the reproductive consequences of pAMH in KARKO offspring to determine whether androgens were mediating this phenotype and where they might be acting. We found that nearly every pAMH-induced deficit present in controls was eliminated in their KARKO littermates. By determining the necessity of AR in kisspeptin cells to induce pAMH phenotypes, we have advanced understanding of the interactions between AMH and androgens in the context of prenatal exposure.

MATERIALS AND METHODS

Mice and pAMH treatment

Mice were group-housed on a 12:12 light/dark cycle with *ad libitum* standard chow diet and water in a temperature-controlled room. All experimental procedures were approved by the University of California, San Diego Institutional Animal Care and Use Committee.

Initial characterization of first (F_1) and second (F_2) generation pAMH offspring was completed using PER2::LUC transgenic mice (RRID:IMSR_JAX:006852) (48) maintained in our local colony on a C57BL/6 background. Mice with the PER2::LUC transgene are viable and fertile with no developmental or morphological differences compared to wildtype littermates (48, 49).

To generate pAMH offspring, virgin adult females (3-4 months old) were paired with adult males (3-4 months old) and checked for copulatory plug as indication of embryonic day (E) 0.5. Timed-pregnant dams were randomly assigned to receive daily intraperitoneal injections from E16.5-E18.5 of either vehicle (VEH) or 0.12 mg/kg/day AMH (recombinant human MIS/AMH protein, R&D Systems, #1737-MS), as previously reported (25). AMH was reconstituted in stocks of 100 μg/ml according to manufacturer's instructions (4 mM HCl + 0.1% BSA) and diluted into 0.01 M PBS pH 7.4. Dams received different volume injections based on weight (100 μl/10 g). Experimenters were blinded to experimental groups. F_1 offspring of both sexes were born into experimental pAMH or VEH control groups, then weaned at postnatal day (P) 21 to begin reproductive phenotyping. Minimum sample sizes were determined based on previous publications of reductive phenotypes following prenatal hormone exposure (25, 43, 44), and two separate cohorts pAMH and VEH offspring were generated to confirm reproducibility of results.

F$_2$ pAMH and VEH offspring were the product of the first generation fertility assay, in which F$_1$ pAMH and VEH females were paired with experimentally naïve wildtype C57BL/6 males (Envigo). Litters from a random subset (n=4) of pAMH and VEH pairings were kept after weaning and phenotyped.

Generation of the KARKO mouse line is described below.

Virgin adult KARKO (AR$^{flox/flox}$:Kisspeptin^{Cre+}) females (3-4 months old) were set up in timed matings with adult control (AR$^{flox/Y}$:Kisspeptin^{Cre-}) males (3-4 months old), and received AMH or VEH injections as described above. F$_1$ offspring of both sexes and genotypes were born into experimental pAMH or VEH control groups, then weaned at P21 to begin phenotyping. Germline-recombined mice were identified and removed from the experiment.

Generation of KARKO mice

We crossed together a previously established AR-flox mouse (RRID: IMSR_NM-CKO-0010) (50) with a validated Kisspeptin-Cre mouse (RRID: IMSR_JAX:023426) (51) to generate a kisspeptin-specific AR knockout (KARKO) mouse. Offspring were backcrossed to produce AR$^{flox/flox}$:Kisspeptin^{Cre+} female and AR$^{flox/Y}$:Kisspeptin^{Cre+} male (KARKO) conditional knockouts or AR$^{flox/flox}$:Kisspeptin^{Cre-} female and AR$^{flox/Y}$:Kisspeptin^{Cre-} male control mice (Ctrl). KARKO Rosa-tdT reporter mice were generated by crossing KARKO mice with Ai9 Rosa-tdTomato mice (RRID: IMSR_JAX:007909) (52), creating mice in which Kisspeptin-Cre expressing cells were identifiable by tdTomato expression.

For genotyping, genomic DNA was isolated from tail tip at P21 and PCR was run using the following primers: AR-flox: F - GTTGATACCTTAACCTCTGC; R - TTCAGCGGCTCTTTTGAAG. Cre: F - GCATTACCGGTCGTAGCAACGAGTG; R -

GAACGCTAGAGCCTGTTTTGCACGTTC. Rosa-tdTomato: F1-
AAGGGAGCTGCAGTGGAGTA; R1- CCGAAAATCTGTGGGAAGTC; F2 -
GGCATTAAAGCAGCGTATCC; R2 - CTGTTCCTGTACGGCATGG. Germline
recombination in the KARKO line was detected using primers: ARKO: F -
GTTGATACCTTAACCTCTGC; R - CCTACATGTACTGTGAGAGG. Germline
recombination in the KARKO Rosa-tdT line was apparent by a pink hue of the skin.

Assessment of body weight, pubertal onset, and anogenital distance

Body weight (g) was measured at various ages throughout postnatal development.
Beginning after weaning at P21, daily checks were made for pubertal onset as marked by vaginal
opening in females and preputial separation in males. Following vaginal opening, vaginal smears
were sampled daily until cellular composition was consistent with first estrus. Anogenital
distance was measured at P30.

Estrous cycling

For each timepoint assessed for estrous cyclicity (P60, P90, 8 months, 10 months, 12
months), adult mice were sampled by vaginal lavage for 16 consecutive days. The slides with
vaginal smears were stained with 0.1% methylene blue, examined by light microscopy, and stage
of cycle was determined by the composition of cell types present (53). Diestrus (D) was
characterized by the presence of predominantly leukocytes, proestrus (P) by the presence of
mostly nucleated cells, estrus (E) by the predominance of cornified epithelial cells, and metestrus
(M) by the presence of leukocytes with some cornified epithelial cells.

Fertility assays

Starting at P90, VEH and pAMH females were paired with experimentally naïve wildtype C57BL/6 adult males for a period of 90 days. VEH and pAMH males were paired with experimentally naïve wildtype C57BL/6 adult females, and female mates were checked daily for formation of a copulatory plug for 10 days. Following plugging assay period, males were left in their pairing for the completion of a 90-day period. For both sexes, the dates of birth of each litter, number of pups per litter, and total number of litters produced were recorded. Litters were left with their mothers until weaning at P21.

Tissue harvest and histology

All mice were sacrificed with CO_2 or isoflurane inhalation followed by rapid decapitation. A vaginally smear was collected from females and sacrificed during diestrus. Trunk blood was collected. One ovary was dissected and rapidly frozen on dry ice, then stored at -80˚C. The other ovary and uterus were dissected and fixed in a solution of 10% acetic acid, 30% formaldehyde, and 60% ethanol.

For histological analysis, fixed ovaries were paraffin embedded with the assistance of Reveal Biosciences, Inc (San Diego, CA) and then serially sectioned at 6 µm using a microtome. Following staining with hematoxylin and eosin (Sigma-Aldrich), every fifth section was scored for corpora lutea and maturing follicles. To avoid double counting, only sections including the ovum nucleus were counted. Follicles were binned into pre-/early antral follicles and late antral follicles. Cysts and atretic follicles were also quantified.

Hormone assays

Trunk blood collected at the time of sacrifice was allowed to clot for 90 minutes at room temperature. Samples were centrifuged at 2,000 rpm for 20 minutes, and sera were transferred to a fresh tube and stored at -80°C. LH and FSH levels were measured using MILLIPLEX MAP Mouse Pituitary Magnetic Bead Kit (Millipore Sigma) and read on Luminex xMAP (Millipore Sigma). Estradiol (E_2), testosterone (T), and AMH levels were analyzed by RIA at the University of Virginia Center for Research in Reproduction Ligand Assay and Analysis Core (Charlottesville, VA).

Quantitative real-time PCR

Harvested ovaries were flash frozen on dry ice and stored at -80°C. Total RNA was isolated using TRIzol reagent (Ambion) followed by chloroform (Sigma-Aldrich) extraction. RNA was purified using Zymo Clean and Concentrator kit according to manufacturer's instruction, and reverse transcribed using iScript cDNA synthesis kit (Bio-Rad Laboratories). Quantitative real-time PCR was carried out in triplicates of each sample on CFX Connect Real-Time PCR detection system (Bio-Rad Laboratories). *Cyp19a1* expression was detected using validated primers: F- GAGTCTGGATCAGTGGAGAG; R- CACGCTTGCTGCCGAATC. Fold change was calculated by ΔΔCT method, using *H2afz* as the control housekeeping gene: F-TCACCGCAGAGGTACTTGAG; R- GATGTGTGGGATGACACCA.

Immunohistochemistry, microscopy, and image analysis

Brains from KARKO Rosa-tdT reporter mice were harvested and fixed in 4% paraformaldehyde solution overnight, then transferred to 30% sucrose. 40 μM sections containing the arcuate nucleus of the hypothalamus were sectioned using a cryostat and

transferred to PBS. Following antigen retrieval in 1X Citra buffer (Biogenex). Sections were washed, then blocked in PBS-T with 5% normal goat serum (Sigma) for 1hr at room temperature before incubation with primary AR antibody (1:50, rabbit polyclonal, Abcam Cat# ab74272, RRID:AB_1280747) at 4˚C overnight. Sections were washed again and incubated in Alexa Fluor 488 secondary antibody (1:100, goat anti-rabbit, Thermo Fisher Scientific Cat# A-11008, RRID:AB_143165) for 30 minutes. Sections were washed and mounted, then coverslipped with ProLong with DAPI (Invitrogen).

Fluorescent microscopy was performed at the University of California, San Diego, Nikon Imaging Core using a Nikon Eclipse Ti2-E microscope with Plan Apo objectives. Samples were excited by the Lumencor SpectraX and acquired with a DS-Qi2 CMOS camera using NIS-Elements software. Lighting was determined by using the minimum LED intensity and exposure time for each channel using positive and negative control slides, and then used for all subsequent acquisition. Images were imported into FIJI (NIH ImageJ). TdTomato-marked kisspeptin expressing cells and cells positive for AR protein expression were counted manually, using FIJI Cell Counter tool.

Statistics

Statistical analyses were performed using Prism 9 (GraphPad) as indicated in the figure legends, with $p < 0.05$ indicated by an asterisk (*), $p < 0.01$ by (**), $p < 0.001$ by (***), and $p < 0.0001$ by (****). Bars in all figures represent means ± SEM. Unpaired t tests were used to compare two treatment groups. Data was assessed for Gaussian distribution by Shapiro-Wilk normalcy test, and when a non-normal distribution was indicated, a nonparametric Mann-Whitney test was performed. When comparing two variables (e.g. treatment and time, treatment

11

and age, treatment and sex, treatment and genotype), a Two-way ANOVA was used and

significant interactions were resolved using Sidak's multiple comparisons test.

RESULTS

CHAPTER 1: PRENATAL AMH EXPOSURE RESULTS IN ROBUST REPRODUCTIVE

DEFICITS ACROSS THE LIFESPAN OF OFFSPRING

To examine the effect of prenatal AMH (pAMH) exposure, wildtype pregnant dams received intraperitoneal injections of AMH or vehicle (VEH) during the late gestational period, as previously reported (25). First generation (F_1) pAMH or VEH offspring were assessed for reproductive phenotypes beginning after weaning (***Figure 1.1***).

F_1 pAMH females exhibit signs of dysregulated reproductive axis throughout the lifespan

We began with phenotypes that had been previously reported to confirm the reproducibility of the model. Consistent with previous findings, F_1 pAMH female offspring showed significantly increased anogenital distance at postnatal day (P)30 (***Figure 1.2a***), indicative of *in utero* androgen exposure. pAMH females exhibited significant delays in puberty as measured by vaginal opening (***Figure 1.2b***) and time to first estrus (***Figure 1.2c***). First estrus was not merely shifted due to the delayed pubertal onset, as there was also a prolonged period in between the onset of puberty and first estrus (***Figure 1.2d***). To measure fecundity, we performed a 90-day fertility assay, in which pAMH females paired with experimentally naïve males showed no delays in time to first litter (***Figure 1.2e***) and normal litter sizes (***Figure 1.2f***) compared to VEH. As previously reported, the number of litters throughout the assay was significantly decreased, including a few pAMH females that failed to produce any litters (***Figure 1.2g***). To increase the temporal resolution of the assay, we examined each month of the assay separately. We found no deficits until after the first 30 days of the assay, when pAMH females were older and produced increasingly fewer litters over time (***Figure 1.2h***).

We next evaluated estrous cyclicity across the lifespan (*Figure 1.3a*). As some pAMH mice did not reach first estrus until P45-55, we began our assessment at P60, which was the beginning of the range previously reported (25). At P60, pAMH females had significantly fewer cycles in a 16-day period (*Figure 1.3b*) and longer cycle length (*Figure 1.3c*). pAMH mice rarely entered pre-/ovulatory proestrus and estrus stages, and spent significantly more time in diestrus/metestrus stages (*Figure 1.3d*). Interestingly, these cycling deficits were ameliorated by P90 (*Figure 1.3a-c, e*), consistent with our fertility assay findings that pAMH mice have a brief window of normal reproductive capacity around 3 months of age. Because prenatal androgen exposure can advance reproductive aging (44), we evaluated estrous cyclicity at 8-12 months of age. At 8 months of age, pAMH females exhibited cycling patterns identical to deficits observed at P60, and distinct from those expected in reproductive senescence (54), significantly fewer cycles during the evaluation period (*Figure 1.3b*), longer cycle length (*Figure 1.3c*), less time in proestrus/estrus, and more time in diestrus/metestrus (*Figure 1.3f*). These pAMH-induced deficits persisted into 10 months of age (*Figure 1.3a-c, g*). By 12 months of age, mice exhibited prolonged estrus patterns consistent with reproductive senescence (54) and were statistically no different from VEH controls (*Figure 1.3a-c, h*).

We harvested blood and reproductive tissues at two timepoints: 5 months of age, when fertility had again begun to decline in pAMH females, and 10 months of age to capture late adulthood effects. We assessed ovarian morphology for markers of ovulation, as well as follicular maturation. At 5 months of age, pAMH ovaries showed significantly decreased number of corpora lutea (*Figure 1.4a, c*) and late antral follicles (*Figure 1.4a, d*). No cystic follicles were observed, and there were no significant differences in the number of pre-/early antral follicles or atretic follicles (data not shown). Gross examination of the female reproductive tract

revealed significantly smaller uteri (***Figure 1.4b, e***) and ovaries (***Figure 1.4b, f***) in pAMH compared to VEH. Although pAMH-induced decreased uterine and ovarian weights persisted until 10 months of age, no significant differences were observed in the number of corpora lutea or late antral follicles at this timepoint. We also found decreased ovarian expression of *Cyp19a1*, which encodes the aromatase enzyme that converts androgens to estrogens (***Figure 1.4g***). No changes in *Ar* or *Amhr2* mRNA expression were observed (***Figure 1.4h-i***).

Finally, we examined serum levels of pituitary gonadotropins and sex steroid hormones at 5 and 10 months of age (***Figure 1.4j-n***). At 5 months, LH was significantly increased and follicle-stimulating hormone (FSH) was significantly decreased in pAMH females compared to VEH. Consistent with decreased uterine weight and aromatase expression, estradiol was decreased and testosterone was increased at this time point. AMH levels in pAMH females were also significantly elevated. Notably, this hormonal profile was not maintained at 10 months of age, when we observed significant reversals of these patterns. At the late adulthood timepoint, pAMH females had significantly decreased LH, testosterone, and AMH levels. There was a trend toward decreased estradiol, but no difference in FSH were observed between pAMH and VEH at 10 months.

F_1 pAMH male offspring also show significant reproductive deficits

Because an androgenic environment *in utero* has been linked to neuroendocrine disruption in males (55, 56), first generation (F_1) male offspring were generated and phenotyped concurrently with their female littermates. No differences in anogenital distance were observed between pAMH and VEH males (***Figure 1.5a***). As with the females, pAMH induced significant delays in pubertal onset in male offspring, as measured by preputial separation (***Figure 1.5b***).

Copulation of pAMH vs. VEH males was measured in a 10-day plugging assay. Whereas all VEH males plugged within 4 days, pAMH males showed significant delays and several did not plug by the 10-day cut-off (*Figure 1.5c*). The pAMH-induced latency to plug did not result in an increased time to first litter in a subsequent 90-day fertility assay (*Figure 1.5d*). Although litter size was also normal (*Figure 1.5e*), pAMH did significantly decrease the number of litters produced in the duration of the assay (*Figure 1.5f*). We found no differences in testis weights (*Figure 1.5g-h*). Serum LH (*Figure 1.5i*) and testosterone (*Figure 1.5j*) levels did not differ, but FSH was significantly decreased at 5 months of age (*Figure 1.5k*). FSH levels normalized by 10 months of age.

In both sexes, pAMH did not induce significant body weight changes at any of the timepoints assayed (*Figure 1.6a-b*).

Figures
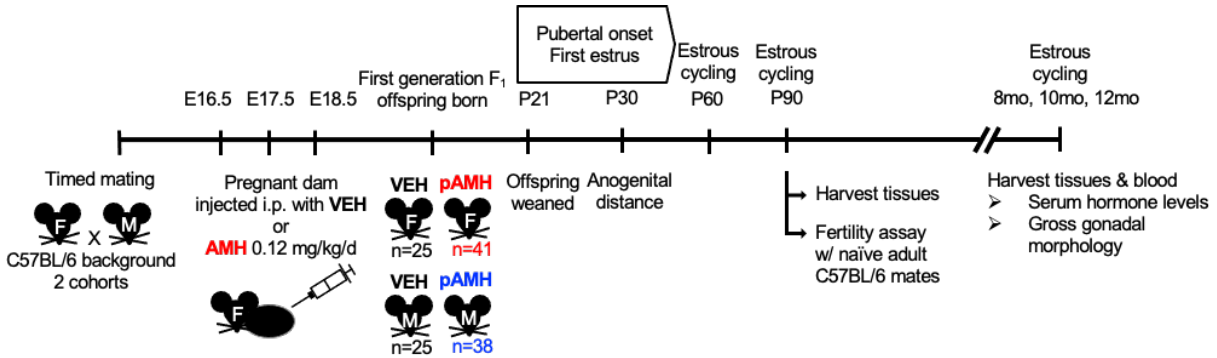
Figure 1.1: Generation of F$_1$ offspring and experimental design. Schematic of experimental design. Pregnant dams on a C57BL/6 background received injections of either AMH or vehicle (VEH) on embryonic days (E)16.5, 17.5 and 18.5. First generation F$_1$ offspring were born into treatment groups (VEH or pAMH) for both sexes (F and M), weaned at postnatal day (P) 21, and examined for reproductive phenotypes. One cohort was sacrificed at 5 months of age, while the other was sacrificed at 10 months of age.
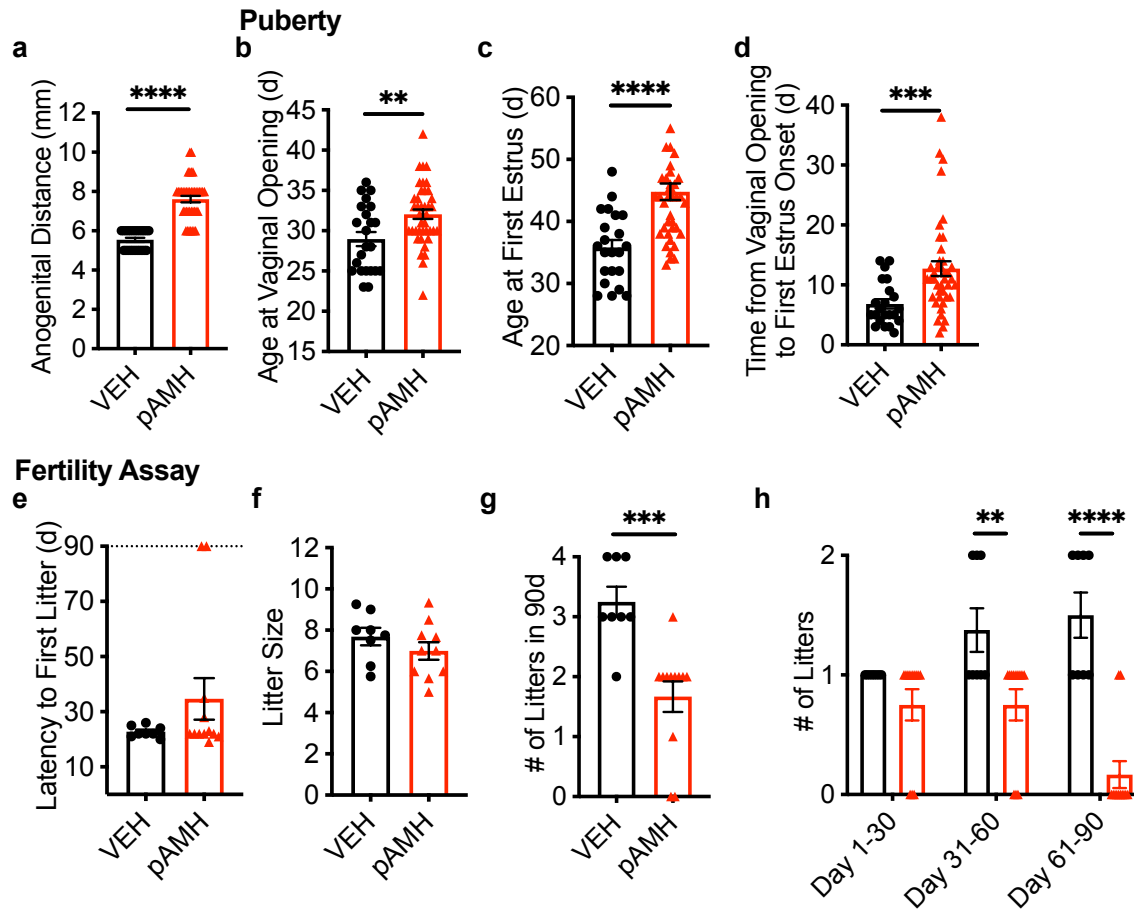
Figure 1.2: Assessment of pAMH-induced phenotypes in F$_1$ female offspring. (a) Anogenital distance in F$_1$ VEH (black, n=25) and pAMH (red, n=41) females was measured at P30 (p<0.0001, 95% CI [5.327, 5.757] vs. [7.280, 7.940]). Assessment for pubertal onset began at P21, as measured by **(b)** time to vaginal opening (p=0.0095, 95% CI [27.15, 30.76] vs. [30.86, 33.24]), **(c)** time to first estrus (p<0.0001, 95% CI [33.31, 38.32] vs. [42.09, 47.47]), and **(d)** time between vaginal opening and first estrus (p=0.0004, 95% CI [5.190, 8.447] vs. [10.24, 15.23]). In a 90-day fertility assay beginning at 3 months of age, F$_1$ VEH (n=8) and pAMH (n=12) were paired with naïve C57BL/6 males to be assessed for **(e)** latency to first litter (p=0.5495, 95% CI [21.03, 24.47] vs. [18.03, 51.30]), **(f)** average litter size per female (p=0.2449, 95% CI [6.677, 8.698] vs. [6.024, 7.960]), **(g)** total number of litters produced (p=0.004, 95% CI [2.659, 3.841] vs. [1.103, 2.231]), and **(h)** number of litters produced in each month of the assay. Treatment x Time, $F_{2,54}$=7.812, p=0.0010; Day 1-30 p=0.5060, 95% CI of diff [-0.2350, 0.7350]; Day 31-60 p=0.0074, 95% CI of diff [0.1400, 1.110]; Day 61-90 p<0.0001, 95% CI of diff [0.8483, 1.818]. Dotted line in **(e)** indicates the 90-day fertility assay cut-off. Data were analyzed using **(a-g)** Mann-Whitney test or **(h)** Two-way ANOVA with Sidak's multiple comparisons test. **p<0.01, ***p<0.001, ****p<0.0001.
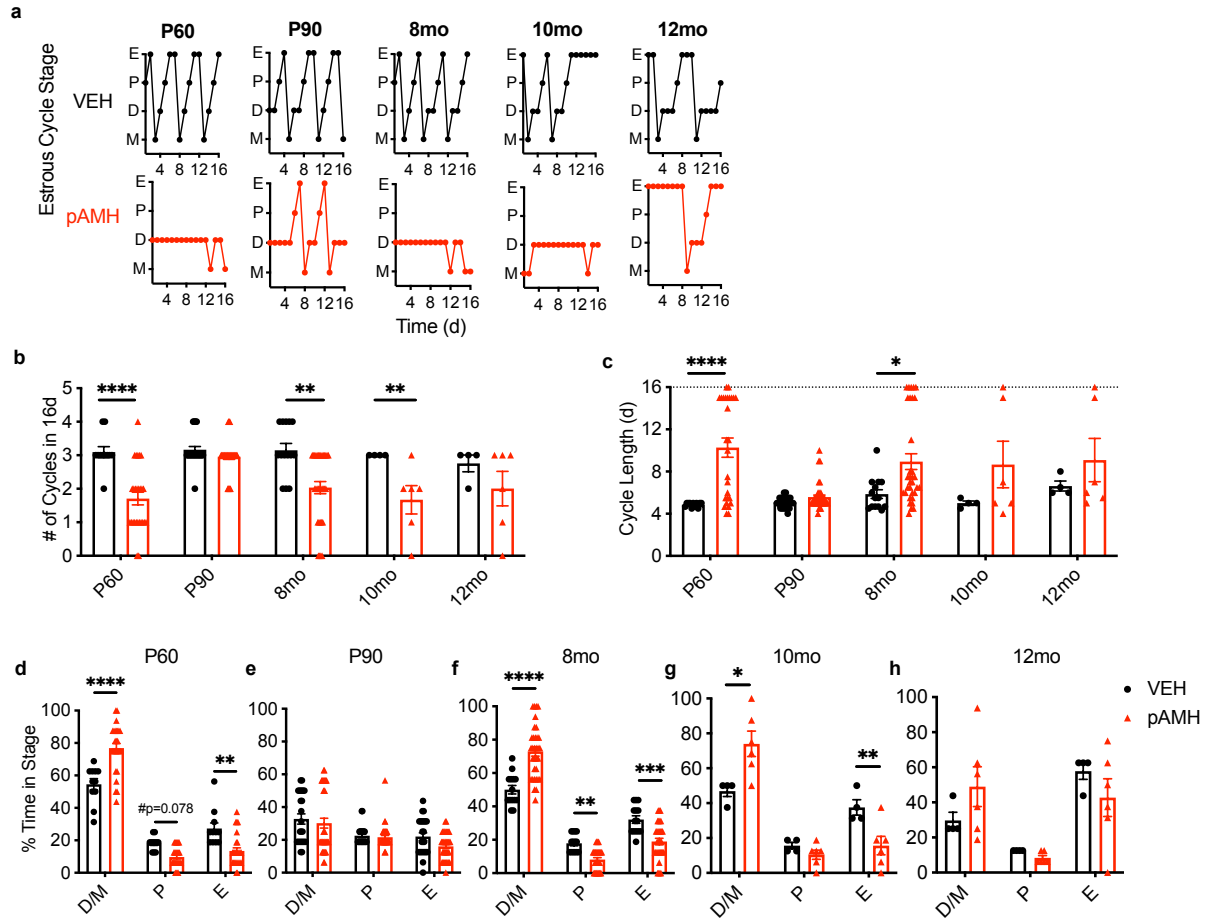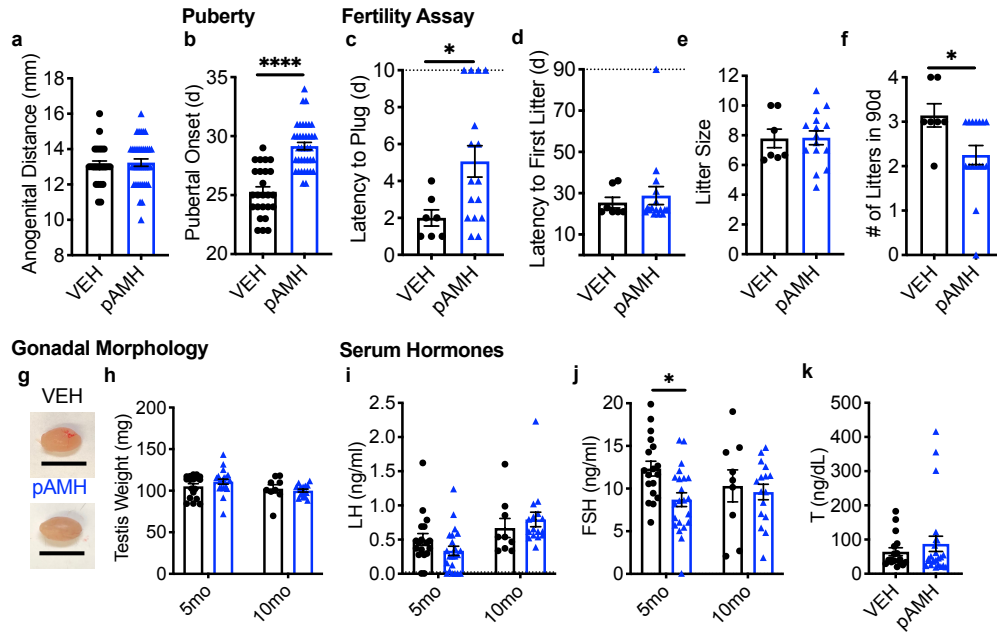
Figure 1.3: pAMH induces significant reproductive phenotypes across the lifespan of first-generation female offspring. (a) Representative estrous cycles of the same VEH (black) and pAMH (red) female offspring at various ages: P60, P90, and 8, 10, and 12 months of age. E, estrus. P, proestrus. D, diestrus. M, metestrus. **(b)** Number of cycles and **(c)** estrous cycle length in the 16-day sampling period at P60 (VEH n=11, pAMH n=27), P90 (VEH n=25, pAMH=41), 8 months (VEH n=14, pAMH n=33), 10 months (VEH n=4, pAMH n=6), and 12 months of age (VEH n=4, pAMH n=6). Dotted line in **(c)** indicates the 16-day cut-off. Number of cycles: Treatment x Age, $F_{4,161}$=3.910, p=0.0047; P60 p<0.0001, 95% CI of diff [0.6523, 2.122]; P90 p=0.8312, 95% CI of diff [-0.3125, 0.7301]; 8mo p<0.0001, 95% CI of diff [0.4573, 1.768], 10mo p=0.0481, 95% CI of diff [0.007199, 2.659], 12mo p=0.5390, 95% CI of diff [-0.5761, 2.076]. Cycle length: Treatment x Age, $F_{4,161}$=3.493, p=0.0092; P60 p<0.0001, 95% CI of diff [-8.309, -2.537]; P90 p=0.9730, 95% CI of diff [-2.562, 1.533]; 8mo p=0.0109, 95% CI of diff [-5.656, -0.5088], 10mo p=0.3009, 95% CI of diff [-8.875, 1.541], 12mo p=0.7143, 95% CI of diff [-0.7666, 2.750]. Percent time spent in each estrous cycle stage during the 16-day sampling period at **(d)** P60 (Treatment x Stage, $F_{2,108}$=26.75, p<0.0001; D/M p<0.0001, 95% CI of diff [-31.45, -13.16]; P p=0.0786, 95% CI of diff [-0.6871, 17.61]; E p=0.0011, 95% CI of diff [4.700, 22.99]), **(e)** P90 (Treatment x Stage, $F_{2,192}$=0.7096, p=0.493), **(f)** 8 months (Treatment x Stage, $F_{2,135}$=33.48, p<0.0001; D/M p<0.0001, 95% CI of diff [-31.24, -14.59]; P p=0.0164, 95% CI of diff [1.389, 18.04]; E p=0.0006, 95% CI of diff [4.879, 21.53]), **(g)** 10 months (Treatment x Stage, $F_{2,24}$=11.77, p=0.0003; D/M p=0.0031, 95% CI of diff [-45.71, -8.471]; P p=0.8587, 95% CI of diff [-13.40, 23.84]; E p=0.0179, 95% CI of diff [3.255, 40.50]), and **(h)** 12 months of age (Treatment x Stage, $F_{2,24}$=2.247, p=0.1275). Data were analyzed using Two-way ANOVA with Sidak's multiple comparisons test. #p<0.1, *p<0.05, **p<0.01, ***p<0.001, ****p<0.0001.

19
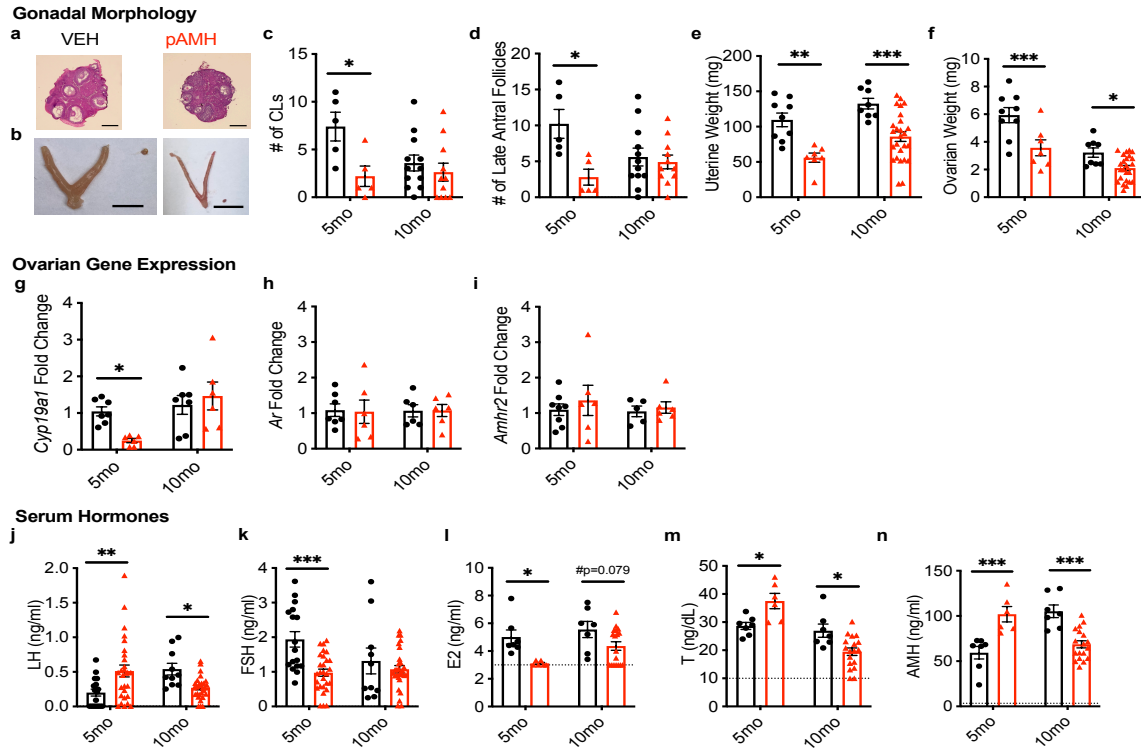
Figure 1.4: pAMH alters gonadal morphology, ovarian gene expression, and serum hormone levels across the lifespan of first-generation female offspring. Representative images from 5-month-old VEH and pAMH female offspring of **(a)** hematoxylin and eosin-stained ovaries (scale bar, 400 µm) and **(b)** harvested uteri and ovaries (scale bar, 1 cm). **(c)** Number of corpora lutea (CLs) (Treatment x Age, $F_{1,29}$=3.576, p=0.0487; 5mo p=0.0193, 95% CI of diff [0.7734, 9.627]; 10mo p=0.6984, 95% CI of diff [-1.975, 3.869]), **(d)** number of late antral follicles (Treatment x Age, $F_{1,29}$=5.607, p=0.0248; 5mo p=0.0081, 95% CI of diff [1.810, 12.99]; 10mo p=0.8909, 95% CI of diff [-3.015, 4.364]), **(e)** uterine weight (Treatment, $F_{1,46}$=26.32, p<0.0001; 5mo p=0.0020, 95% CI of diff [18.33, 88.69]; 10mo p=0.0008, 95% CI of diff [18.35, 74.80]), and **(f)** ovarian weight (Treatment, $F_{1,46}$=20.61, p<0.0001; 5mo p=0.0005, 95% CI of diff [0.9818, 3.742]; 10mo p=0.0493, 95% CI of diff [0.002805, 2.239]) of female offspring at 5 (VEH n=5, pAMH n=5) and 10 (VEH n=12, pAMH n=11) months of age. mRNA expression levels of **(g)** *Cyp19a1* (Treatment x Age, $F_{1,22}$=4.883, p=0.0378; 5mo p=0.0499, 95% CI of diff [0.0002904, 1.594]; 10mo p=0.7257, 95% CI of diff [-1.038, 0.5562]), **(h)** *Ar* (Treatment x Age, $F_{1,22}$=0.01383, p=0.9075; Treatment, $F_{1,22}$=0.007455, p=0.9320), and **(i)** *Amhr2* (Treatment x Age, $F_{1,22}$=0.09367, p=0.7626; Treatment, $F_{1,22}$=0.5490, p=0.4669) from ovaries of VEH (n=7) and pAMH (n=6) female offspring at 5 and 10 months of age. Serum **(j)** LH and **(k)** FSH levels at 5 (VEH n=17, pAMH n=28) and 10 (VEH n=10, pAMH=29) months of age. LH: Treatment x Age, $F_{1,80}$=15.33, p=0.0002; 5mo p=0.0031, 95% CI of diff [-0.5301, -0.09483]; 10mo p=0.0403, 95% CI of diff [0.009950, 0.5291]. FSH: Treatment x Age, $F_{1,80}$=4.206, p=0.0436; 5mo p=0.0001, 95% CI of diff [0.4462, 1.476]; 10mo p=0.6138, 95% CI of diff [-0.3768, 0.8554]. Serum **(l)** estradiol (E2), **(m)** testosterone (T), and **(n)** AMH levels at 5 (VEH n=7, pAMH n=6) and 10 (VEH n=7, pAMH=18) months of age. E2: Treatment, $F_{1,34}$=11.86, p=0.0015; 5mo p=0.0209, 95% CI of diff [0.2587, 3.544]; 10mo p=0.0797, 95% CI of diff [-0.1190, 2.511]. T: Treatment x Age, $F_{1,34}$=16.74, p=0.0002; 5mo p=0.0148, 95% CI of diff [-16.15, -1.579]; 10mo p=0.0103, 95% CI of diff [1.622, 13.29]. AMH: Treatment x Age, $F_{1,34}$=37.71, p<0.0001; 5mo p=0.0003, 95% CI of diff [-66.10, -19.04]; 10mo p=0.0001, 95% CI of diff [17.71, 55.38]. Dotted lines in **(l-n)** indicate sensitivity threshold of the hormone assay. Data were analyzed using Two-way ANOVA with Sidak's multiple comparisons test. #p<0.1, *p<0.05, **p<0.01, ***p<0.001.

Figure 1.5: pAMH induces significant reproductive deficits in male offspring. (a) Anogenital distance in first generation VEH (black, n=25) and pAMH (blue, n=38) males was measured at P30 (p=0.5401, 95% CI [12.58, 13.59] vs. [12.81, 13.67]). Assessment for pubertal onset began at P21, as measured by **(b)** preputial separation (p<0.0001, 95% CI [24.41, 26.15] vs. [28.52, 29.80]). In a 90-day fertility assay beginning at 3 months of age, VEH (n=7) and pAMH (n=16) were mated with naïve C57BL/6 females to be assessed for **(c)** time to plug by a 10-day cut-off indicated by the dotted line (p=0.0302, 95% CI [0.9321, 3.068] vs. [3.243, 6.882]), **(d)** latency to first litter by the 90-day cut-off indicated by the dotted line (p=0.7283, 95% CI [19.02, 31.83] vs. [19.53, 38.09]), **(e)** average litter size per male (p=0.7170, 95% CI [6.258, 9.313] vs. [6.834, 8.832]), and **(f)** total number of litters (p=0.0256, 95% CI [2.505, 3.781] vs. [1.794, 2.706]). **(g)** Representative images from 10-month-old VEH and pAMH male offspring of harvested testes (scale bar, 1 cm). **(h)** Testis weight, **(i)** serum LH, and **(j)** serum FSH of male offspring at 5 (VEH n=18, pAMH n=22) and 10 (VEH n=9, pAMH n=16) months of age. Testis weight: Treatment x Age, $F_{1,61}$=1.403, p=0.2409; Treatment, $F_{1,61}$=0.2694, p=0.6056. LH: Treatment x Age, $F_{1,61}$=2.206, p=0.1427; Treatment, $F_{1,61}$=0.04453, p=0.8336. FSH: Treatment, $F_{1,61}$=4.259, p=0.0433; 5mo p=0.0121, 95% CI of diff [0.7031, 6.562]; 10mo p=0.8917, 95% CI of diff [-3.126, 4.556]. **(k)** Serum testosterone (T) at 10 months of age (VEH n=17, pAMH n=14) (p=0.9687, 95% CI [39.49, 89.05] vs. [41.24, 133.5]). Data were analyzed using **(a-f)** Mann-Whitney test or **(h-k)** Two-way ANOVA with Sidak's multiple comparisons test. *p<0.05, ****p<0.0001.
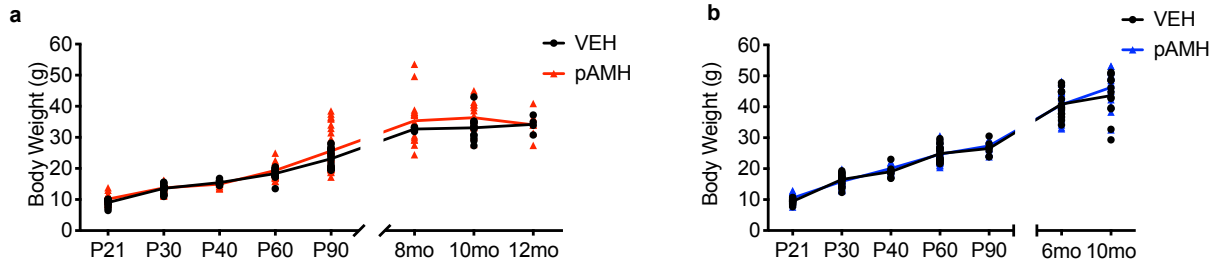
Figure 1.6: pAMH did not significantly affect body weight across the lifespan of first-generation offspring. Body weight measurements at various ages in VEH and pAMH **(a)** F_1 females (Treatment x Age, $F_{7,143} = 1.729$, p=0.1029), **(b)** F_1 males (Treatment x Age, $F_{6,190} = 1.290$, p=0.2638). Data were analyzed using Mixed-effects model with the Geisser-Greenhouse correction to account for differing variability of differences.

CHAPTER 2: PRENATAL AMH-INDUCED REPRODUCTIVE PHENOTYPES ARE

TRANSGENERATIONAL IN BOTH SEXES

The findings of Chapter 1 indicated that prenatal AMH exposure robustly altered the

neuroendocrine reproductive axis for both sexes. Alterations observed extended beyond

previously reported peripubertal and early adult timepoints, and well into late adulthood.

Notably, we found that reproductive-aged F_1 pAMH females had significant alterations in their

hormonal profile. Specifically, elevations in AMH led us to investigate whether second

generation (F_2) offspring of F_1 pAMH females also exhibit reproductive deficits (***Figure 2.1***).

We examined both female and male offspring of the F_2 generation, as both sexes in the F_1

generation were affected.

F_2 pAMH females exhibit signs of dysregulated reproductive axis throughout the lifespan

As in the F_1 generation, F_2 pAMH females had significantly increased anogenital distance

at P30 (***Figure 2.2a***) and robust delays in onset of puberty as measured by vaginal opening

(***Figure 2.2b***), first estrus (***Figure 2.2c***), and the time between vaginal opening and first estrus

(***Figure 2.2d***). In a fertility assay, F_2 pAMH females showed a trend toward decreased number of

litters produced in the 90-day duration (***Figure 2.2e***). pAMH significantly disrupted estrus

cyclicity at P60 and 8 months of age in the F_2 generation (***Figure 2.2f***). At both timepoints, F_2

pAMH females had fewer cycles in a 16-day period (***Figure 2.2g***), longer cycle length (***Figure

2.2h***), and spent significantly more time in the infertile diestrus/metestrus stages (***Figure 2.2i-j***)

compared to F_2 VEH controls. Ovarian morphology at 4 months of age revealed significantly

decreased number of corpora lutea (***Figure 2.3a, c***), and a trend toward decreased number of late

antral follicles (***Figure 2.3a, d***). Ovarian weight was decreased (***Figure 2.3b, e***) at this timepoint,

but there were no changes in uterine weight (*Figure 2.3b, f*) or *Cyp19a1* expression (*Figure 2.3g*). Unlike in the F1 generation, the F_2 generation pAMH females did not have smaller uteri or ovaries at 10 months of age (*Figure 2.3e-f*).

When we measured serum hormone levels in F_2 females, significant changes were found at early timepoints that were ameliorated by late adulthood. Peripubertal gonadotropin levels were significantly altered in F_2 females (*Figure 2.3h-i*), consistent with high LH and low FSH observed in daughters of PCOS women during puberty (57). Elevated LH and decreased FSH was also present at 4 months of age. No differences in estradiol were detected (*Figure 2.3j*), however F_2 pAMH females had significantly increased testosterone (*Figure 2.3k*) and AMH (*Figure 2.3l*) at 4 months. There were no pAMH-induced hormonal changes at 10 months of age (*Figure 2.3h-l*).

F_2 pAMH male offspring also show significant reproductive deficits

In F_2 male offspring, significantly delayed pubertal onset was again found in the pAMH group compared to VEH controls (*Figure 2.4a*). Copulation as measured by time to plug was not significantly affected in the F_2 generation, although 30% of the pAMH group did not plug by the 10-day cut-off (*Figure 2.4b*). Similar to F_2 pAMH females, serum FSH in second generation pAMH males was significantly decreased at P30 and 3 months of age (*Figure 2.4c*).

In both sexes of the F_2 generation, pAMH did not induce significant body weight changes at any of the timepoints assayed (*Figure 2.5a-b*).

Figures
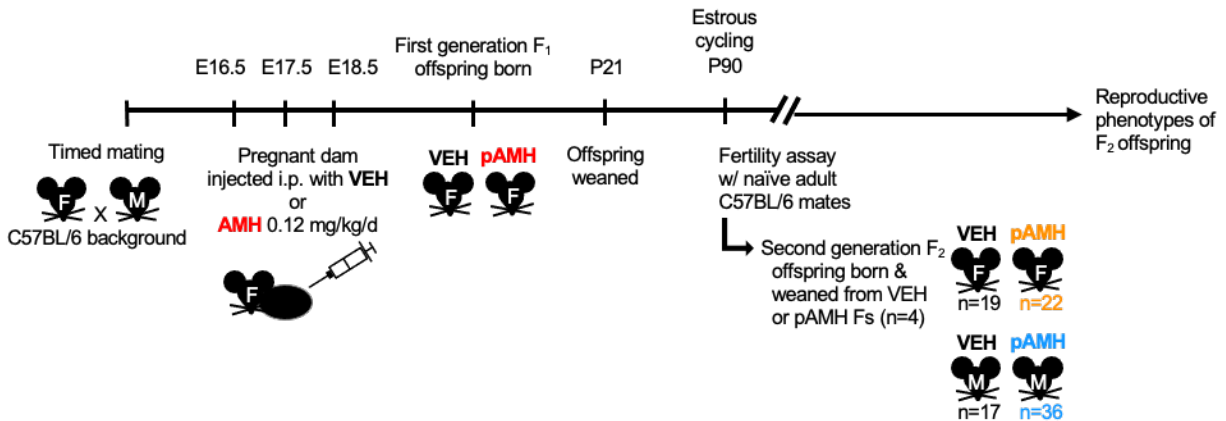
Figure 2.1: Generation of F$_2$ offspring and experimental design. (a) Schematic of experimental design. Pregnant dams on a C57BL/6 background received injections of either AMH or vehicle (VEH) on embryonic days (E)16.5, 17.5 and 18.5. First generation F$_1$ offspring were born into treatment groups (VEH or pAMH) for both sexes (F and M), weaned at postnatal day (P) 21, and examined for reproductive phenotypes. One cohort was sacrificed at 5 months of age, while the other was sacrificed at 10 months of age.
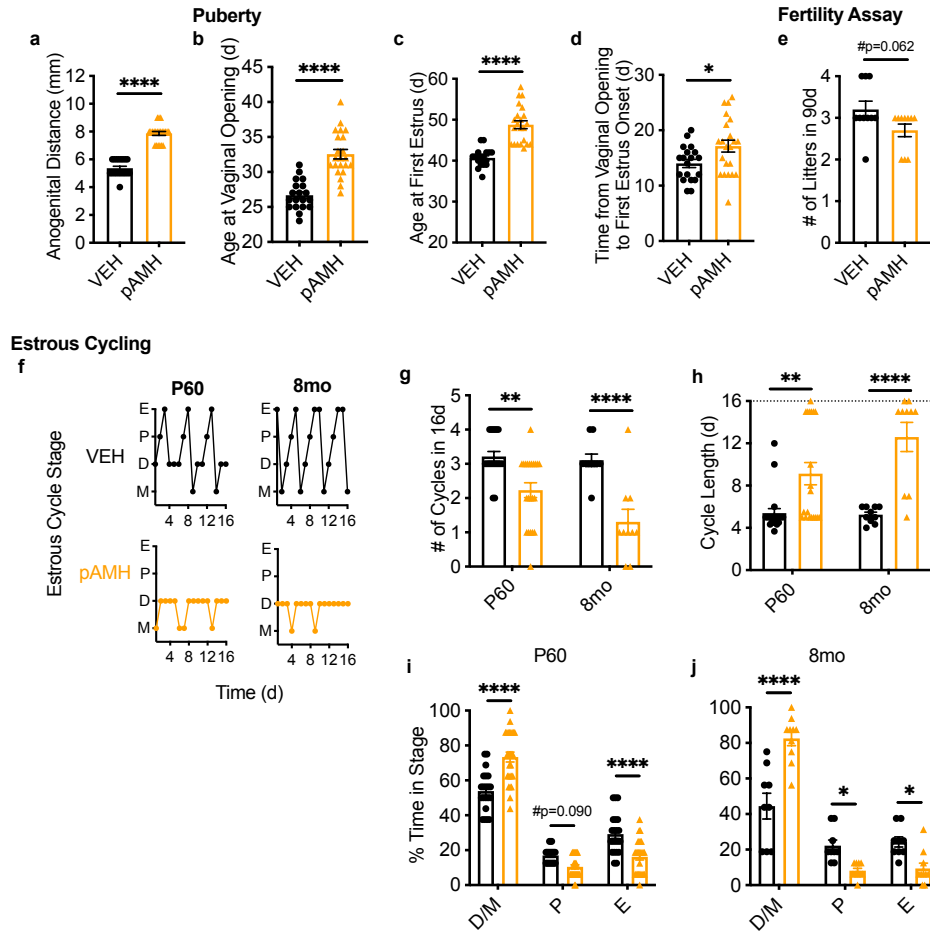
Figure 2.2: pAMH phenotypes extend into second generation F$_2$ female offspring. (a) Anogenital distance in F$_2$ VEH (n=19) and pAMH (n=22) females was measured at P30 (p<0.0001, 95% CI [5.081, 5.656] vs. [7.580, 8.147]). Assessment for pubertal onset began at P21, as measured by **(b)** time to vaginal opening (p<0.0001, 95% CI [25.68, 27.69] vs. [31.13, 33.96]), **(c)** time to first estrus (p<0.0001, 95% CI [39.64, 41.73] vs. [46.76, 50.79]), and **(d)** time between vaginal opening and first estrus (p=.0.0284, 95% CI [12.48, 15.52] vs. [14.89, 19.39]). **(e)** In a fertility assay beginning at 3 months of age, VEH and pAMH F$_2$ females (n=10) were mated with naïve males and assessed for number of litters produced in 90 days (p=0.0624, 95% CI [2.748, 3.652] vs. [2.354, 3.046]). **(f)** Representative estrous cycles of the same F$_2$ VEH and pAMH females at P60 and 8 months of age. E, estrus. P, proestrus. D, diestrus. M, metestrus. Quantification of estrous cycling patterns during the 16-day sampling period at P60 in F$_2$ females (VEH, black, n=19, pAMH, orange, n=22) and 8-month-old F$_2$ females (n=10). **(g)** Number of cycles at P60 and 8 months of age (Treatment, F$_{1,57}$=33.65, p=<0.0001; P60 p=0.0015, 95% CI of diff [0.3511, 1.615]; 8mo p<0.0001, 95% CI of diff [0.8973, 2.703]). **(h)** Estrous cycle length at P60 and 8 months of age (Treatment, F$_{1,57}$=3.725, p<0.0001; P60 p=0.0020, 95% CI of diff [-6.197, -1.260]; 8mo p<0.0001, 95% CI of diff [-10.88, -3.817]). Percent time spent in each estrous cycle stage **(i)** at P60 (Treatment x Stage, F$_{2,138}$=32.69, p<0.0001; D/M p<0.0001, 95% CI of diff [-29.78, -12.24]; P p=0.0907, 95% CI of diff [-0.7231, 13.82]; E p<0.0001, 95% CI of diff [5.692, 20.23]) and **(j)** 8 months of age (Treatment x Stage, F2,51=29.65, p=<0.0001; D/M p<0.0001, 95% CI of diff [-51.62, -24.29]; P p=0.0431, 95% CI of diff [0.3348, 27.86]; E p=0.0295, 95% CI of diff [1.168, 28.69]). Dotted line in **(h)** indicates the 16-day cut-off. Data were analyzed using **(a-e)** Mann-Whitney test or **(g-j)** Two-way ANOVA with Sidak's multiple comparisons test. #p<0.1, *p<0.05, **p<0.01, ***p<0.001, ****p<0.0001.
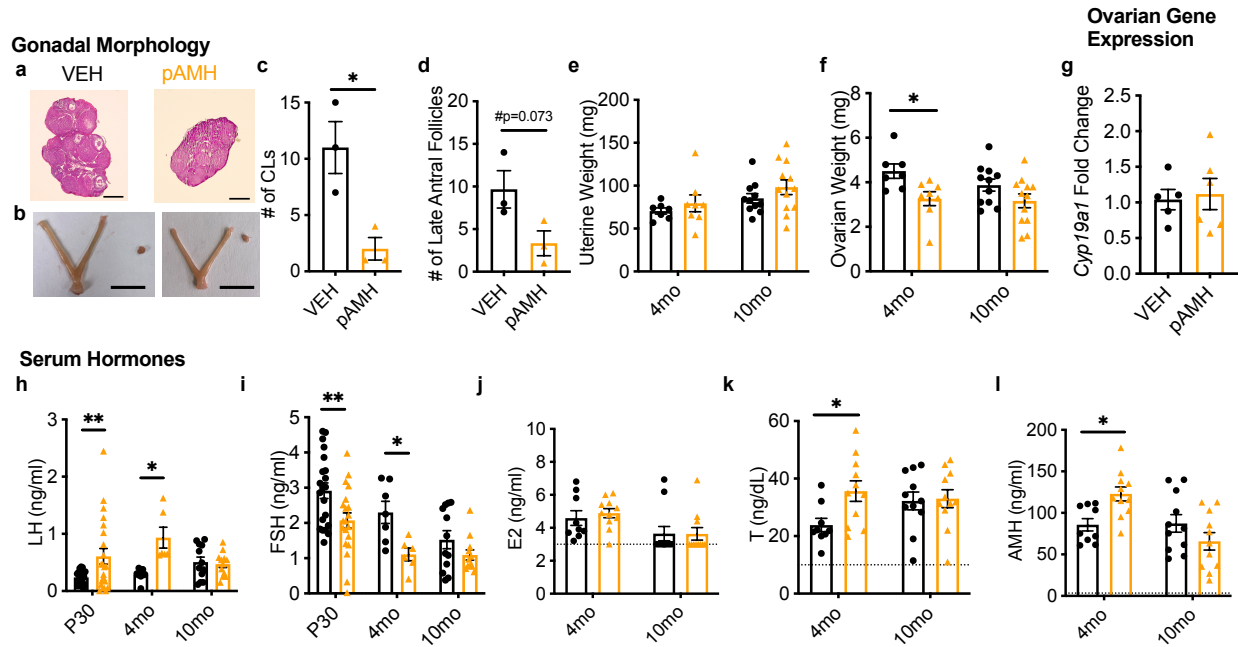
Figure 2.3: Alterations in gonadal morphology and serum hormones in second generation F₂ pAMH females are no longer present in late adulthood. Representative images from 4-month-old F₂ VEH and pAMH females of **(a)** hematoxylin and eosin-stained ovaries (scale bar, 400 μm) and **(b)** harvested uteri and ovaries (scale bar, 1 cm). Number of **(c)** corpora lutea (CLs) (p=0.0232, 95% CI [1.063, 20.94] vs. [-2.303, 6.303]) and **(d)** late antral follicles (p=0.0733, 95% CI [0.2619, 19.07] vs. [-2.918, 9.585]) in 4-month-old F₂ VEH and pAMH (n=3). **(e)** Uterine weight (Treatment x Age, $F_{1,34}$=0.06281, p=0.8036; Treatment, $F_{1,34}$=1.943, p=0.1723) and **(f)** ovarian weight (Treatment, $F_{1,34}$=9.523, p=0.0040; 4mo p=0.0326, 95% CI of diff [0.09057, 2.384]; 10mo p=0.1592, 95% CI of diff [-0.2190, 1.631]) of F₂ females at 4 (n=7-8) and 10 (n=11-12) months of age. **(g)** mRNA expression levels of *Cyp19a1* from F₂ ovaries at 4 months of age (n=5-6, p>0.9999, 95% CI [0.6448, 1.435] vs. [0.5545, 1.682]). Serum levels of **(h)** LH and **(i)** FSH at P30 (n=19-22), 4 (n=6-7) and 10 (n=12) months of age. LH: Treatment x Age, $F_{2,72}$=3.496, p=0.0356; P30 p=0.0129, 95% CI of diff [-0.6729, -0.06268]; 4mo p=0.0135, 95% CI of diff [-1.192, -0.1082]; 10mo p=0.9955, 95% CI of diff [-0.3638, 0.4317]. FSH: Treatment x Age, $F_{2,72}$=0.8605, p=0.4272; P30 p=0.0082, 95% CI of diff 0.1793, 1.510]; 4mo p=0.0480, 95% CI of diff [0.007765, 2.378]; 10mo p=0.5348, 95% CI of diff [-0.4343, 1.305]. Serum **(j)** estradiol (E2), **(k)** testosterone (T), and **(l)** AMH levels at 4 and 10 months of age (n=9-11). E2: Treatment x Age, $F_{1,38}$=0.1656, p=0.6863; Treatment, $F_{1,38}$=0.1399, p=0.7104. T: Treatment x Age, $F_{1,38}$=3.041, p=0.0493; 4mo p=0.0278, 95% CI of diff [-22.46, -1.134]; 10mo p=0.9796, 95% CI of diff [-10.91, 9.330]. AMH: Treatment x Age, $F_{1,38}$=9.440, p=0.0039; 4mo p=0.0217, 95% CI of diff [-69.49, -4.841]; 10mo p=0.2057, 95% CI of diff [-9.030, 52.27]. Dotted lines in **(j-l)** indicate sensitivity threshold of the hormone assay. **(u)** Pubertal onset in F₂ VEH (black, n=19) and pAMH (light blue, n=22) males as measured by preputial separation (p=0.0011, 95% CI [27.92, 31.25] vs. [31.35, 33.04]). **(v)** Time to plug in F₂ VEH and pAMH males by a 10-day cut-off, indicated by the dotted line (n=10, p=0.4186, 95% CI [1.841, 5.359] vs. [2.580, 8.020]). **(w)** Serum FSH levels at P30 (VEH n=17, pAMH n=28) and 3 (VEH n=17, pAMH n=28) months of age in F₂ males. FSH: Treatment, $F_{1,85}$=19.06, p<0.0001; P30 p=0.0201, 95% CI of diff [0.4623, 6.386]; 3mo p=0.0014, 95% CI of diff [1.716, 8.010]. Data were analyzed using **(c-d, g)** Mann-Whitney test or **(e-f, h-l)** Two-way ANOVA with Sidak's multiple comparisons test. #p<0.1, *p<0.05, **p<0.01.
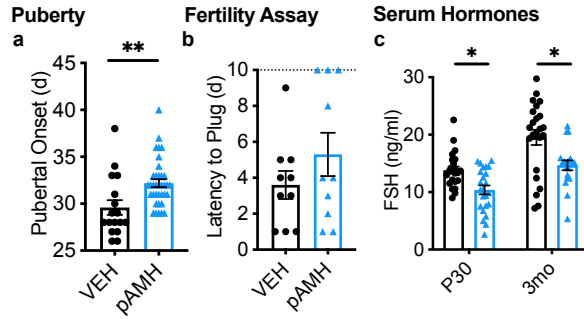
Figure 2.4: pAMH phenotypes extend into second generation F$_2$ male offspring. (a) Pubertal onset in F$_2$ VEH (black, n=19) and pAMH (light blue, n=22) males as measured by preputial separation (p=0.0011, 95% CI [27.92, 31.25] vs. [31.35, 33.04]). **(b)** Time to plug in F$_2$ VEH and pAMH males by a 10-day cut-off, indicated by the dotted line (n=10, p=0.4186, 95% CI [1.841, 5.359] vs. [2.580, 8.020]). **(c)** Serum FSH levels at P30 (VEH n=17, pAMH n=28) and 3 (VEH n=17, pAMH n=28) months of age in F$_2$ males. FSH: Treatment, $F_{1,85}$=19.06, p<0.0001; P30 p=0.0201, 95% CI of diff [0.4623, 6.386]; 3mo p=0.0014, 95% CI of diff [1.716, 8.010]. Data were analyzed using **(a-b)** Mann-Whitney test or **(c)** Two-way ANOVA with Sidak's multiple comparisons test. *p<0.05, **p<0.01.
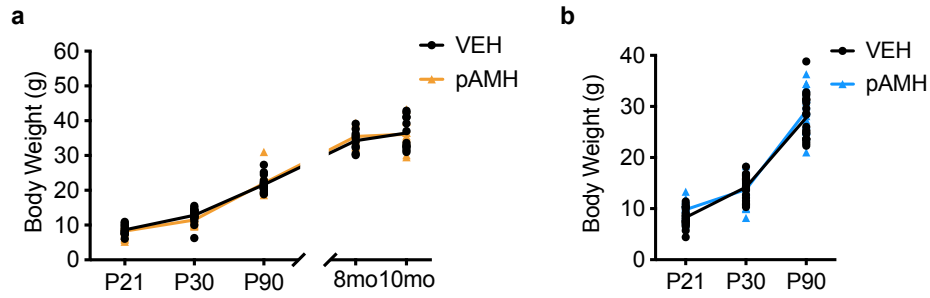
Figure 2.5: pAMH did not significantly affect body weight across the lifespan of first-generation offspring. Body weight measurements at various ages in VEH and pAMH **(a)** F_2 females (Treatment x Age, $F_{4,111}= 1.374$, $p=0.2476$), **(b)** F_2 males (Treatment x Age, $F_{2,149}= 1.729$, $p=0.1366$). Data were analyzed using Mixed-effects model with the Geisser-Greenhouse correction to account for differing variability of differences.

CHAPTER 3: ANDROGEN RECEPTOR IN KISSPEPTIN CELLS IS NECESSARY FOR
PRENATAL AMH-INDUCED PHENOTYPES

Our findings in Chapters 1 and 2 demonstrated that prenatal AMH exposure has lasting effects on offspring of both sexes and that resulting alterations could be carried on into the subsequent generation. After characterizing a full profile of pAMH-induced reproductive phenotypes, we next sought to probe at a possible androgen-mediated mechanism.

To test our hypothesis that pAMH-induced phenotypes are mediated by androgen signaling at the level of kisspeptin cells, we generated a kisspeptin-specific AR knockout (KARKO) mouse line by crossing together previously established AR-flox (50) and Kisspeptin-Cre mice (51). Exon 2 of the Ar gene is flanked by LoxP sites, allowing for the functional AR protein to be present in $AR^{flox/flox}$ females and $AR^{flox/Y}$ males (Ctrl) and excised in $AR^{flox/flox}$:Kisspeptin^{Cre+} females and $AR^{flox/Y}$:Kisspeptin^{Cre+} males (KARKO). Specificity of the knockout was confirmed by crossing this KARKO mouse line with a Rosa-tdTomato reporter mouse line to visualize kisspeptin-expressing cells, followed by immunohistochemistry on sections containing the ARC region of hypothalamus and determined colocalization of AR to kisspeptin-expressing cells (***Figure 3.1a***). Compared to littermate controls ($AR^{flox/flox}$ females and $AR^{flox/Y}$ males), KARKO mice of both sexes had drastic reductions in the percentage of kisspeptin-expressing cells containing AR in the ARC (***Figure 3.1b***).

All pAMH phenotypes were eliminated in female KARKO offspring

After confirming the successful recombination of the AR-flox allele in kisspeptin-expressing cells, we generated F_1 pAMH offspring in the KARKO mouse line. Pregnant KARKO dams were injected with AMH or VEH late in gestation, then offspring of both

genotypes (KARKO vs. Ctrl) and sexes were born and assessed for pAMH-induced phenotypes after weaning (*Figure 3.2*). Importantly, we observed no statistical differences between KARKO and Ctrl within the VEH group on any measure, indicating that AR knockout in kisspeptin cells alone is insufficient to cause significant reproductive deficits in either males or females.

As in our first set of experiments, pAMH significantly increased anogenital distance in Ctrl females (*Figure 3.3a*). However, in KARKO females, there was no difference between VEH and pAMH groups. Similarly, pAMH delayed the onset of puberty in Ctrl, but not KARKO females, as measured by vaginal opening (*Figure 3.3b*), first estrus (*Figure 3.3c*), and prolonged time between them (*Figure 3.3d*). pAMH decreased the number of litters in a fertility assay for Ctrl, but had no effect in the KARKO group (*Figure 3.3e*). Estrous cyclicity was significantly disrupted in Ctrl pAMH females at P60 and 8 months of age, but no differences were observed between KARKO pAMH and KARKO VEH (*Figure 3.3f-l*). At 10 months of age, pAMH-induced decreases in uterine weight (*Figure 3.4a*), ovarian weight (*Figure 3.4b*), LH (*Figure 3.4c*), testosterone (*Figure 3.4d*), and AMH (*Figure 3.4e*) were all present in Ctrl but not KARKO females. KARKO effects on all significant pAMH-induced phenotypes in females are summarized below (*Table 3.1*).

All but one of the pAMH phenotypes were eliminated in male KARKO offspring

In males, we saw similar pAMH-induced pubertal delays in Ctrl but not KARKO (*Figure 3.5a*). Interestingly, plugging behavior was significantly delayed by pAMH in both Ctrl and KARKO (*Figure 3.5b*). This was the only pAMH-induced phenotype assayed in either sex that was not eliminated in the KARKO group. Consistent with our prior experiment, no statistical differences were found on latency to first litter (*Figure 3.5c*) or litter size (*Figure 3.5d*). The

number of litters produced during the duration of the assay was significantly reduced in Ctrl pAMH vs. Ctrl VEH, but not in KARKO males (*Figure 3.5e*). KARKO effects on all significant pAMH-induced phenotypes in males are summarized below (*Table 4.2*).

Body weight was unchanged at all of the timepoints assayed regardless of treatment in both sexes of both genotypes (*Figure 3.6a-b*).

Figures
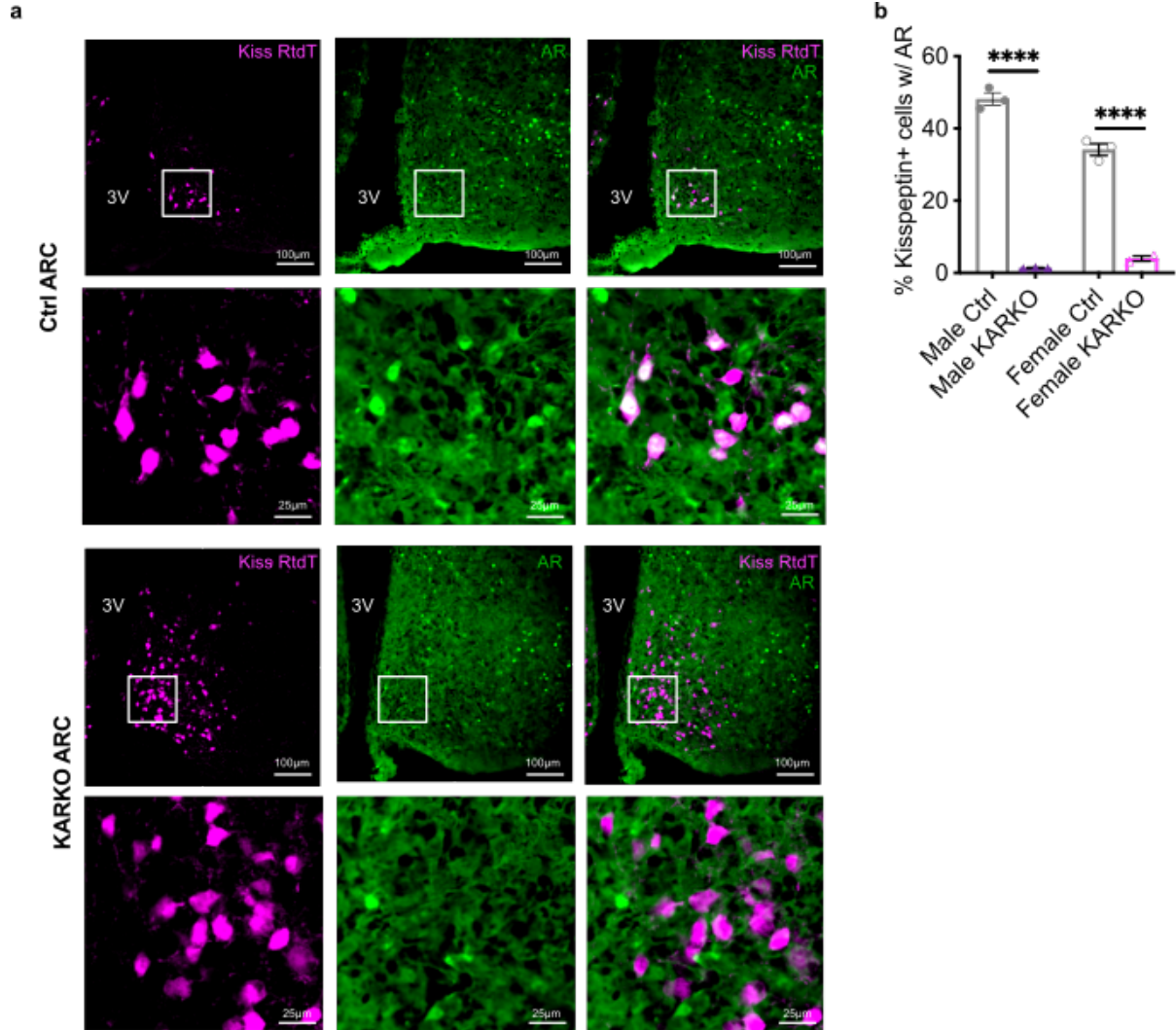
Figure 3.1: Confirmation of androgen receptor knockout in kisspeptin neurons of KARKO mice.
(a) Representative fluorescent images of the arcuate nucleus (ARC) in adult males from the KARKO Rosa-tdTomato reporter line. Colocalization (white) of kisspeptin Rosa-tdTomato (Kiss RtdT, magenta) and androgen receptor (AR, green) is apparent in Ctrl but not KARKO sections. Localization of AR to the nucleus is well visualized given the high circulating testosterone levels in males. **(b)** Percent of kisspeptin-expressing cells with AR in Ctrl and KARKO males and females (n=3). Genotype x Sex, $F_{1,7}$=37.62, p=0.0005; Males p<0.0001, 95% CI of diff [41.62, 51.84]; Females p<0.0001, 95% CI of diff [24.42, 35.85]. Data were analyzed using Two-way ANOVA with Sidak's multiple comparisons test. ****p<0.0001.
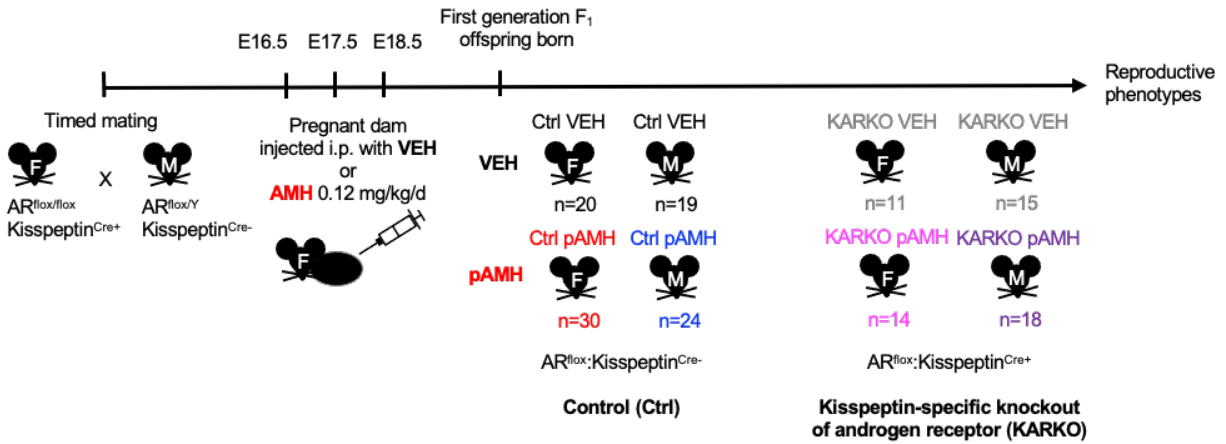
Figure 3.2: **Generation of pAMH offspring in KARKO mouse line.** Timed matings between AR$^{flox/flox}$ Kisspeptin^{Cre+} (KARKO) females and AR$^{flox/Y}$ Kisspeptin^{Cre-} (Ctrl) males were set up and dams received either VEH or AMH injections on embryonic days (E)16.5, 17.5 and 18.5. Offspring were born into treatment groups (VEH or pAMH) for both sexes (F and M), in both genotypes (Ctrl and KARKO).
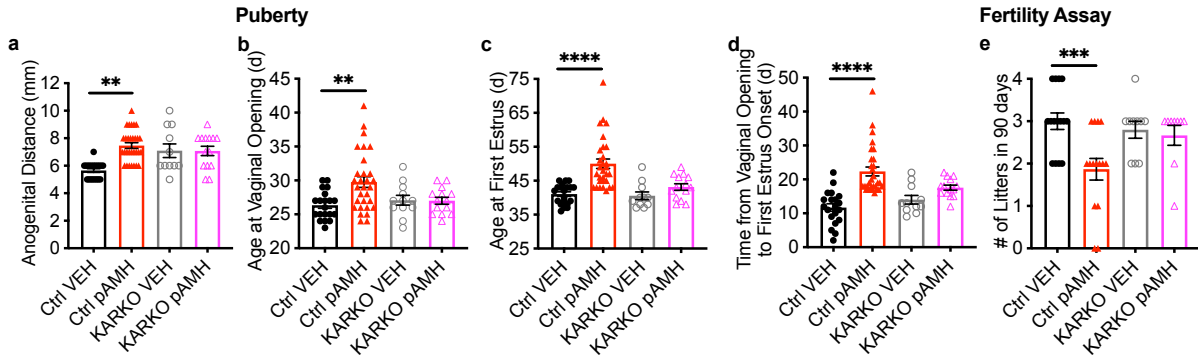
Figure 3.3: pAMH failed to induce reproductive phenotypes in KARKO female offspring. (a) Anogenital distance measurements at P30 in Ctrl (VEH, black, n=20, pAMH, red, n=30) and KARKO (VEH, gray, n=11, pAMH, magenta, n=14) females (Treatment x Genotype, $F_{1,72}$=10.61, p=0.0017; Ctrl p<0.0001, 95% CI of diff [-2.567, -1.066]; KARKO p=0.9989, 95% CI of diff [-1.028, 1.067]). Assessment for pubertal onset began at P21, as measured by **(b)** time to vaginal opening (Treatment x Genotype, $F_{1,72}$=5.000, p=0.0284; Ctrl p=0.0009, 95% CI of diff [-5.532, -1.302]; KARKO p=0.9972, 95% CI of diff [-2.799, 2.966]), **(c)** time to first estrus (Treatment x Genotype, $F_{1,71}$=5.462, p=0.0223; Ctrl p<0.0001, 95% CI of diff [-12.57, -5.333]; KARKO p=0.4260, 95% CI of diff [-7.646, 2.451]), and **(d)** time between vaginal opening and first estrus (Treatment x Genotype, $F_{1,71}$=6.527, p=0.0128; Ctrl p<0.0001, 95% CI of diff [-14.31, -6.955]; KARKO p=0.2193, 95% CI of diff [-8.705, 1.562]). **(e)** In a fertility assay beginning at 3 months of age, Ctrl (VEH n=15, pAMH n=15) and KARKO (VEH n=10, pAMH n=9) were assessed for number of litters produced in 90 days (Treatment x Genotype, $F_{1,45}$=4.454, p=0.0404; Ctrl p=0.0008, 95% CI of diff [0.4513, 1.815]; KARKO p=0.9221, 95% CI of diff [-0.7249, 0.9916]). Data were analyzed using Two-way ANOVA with Sidak's multiple comparisons test. **p<0.01, ***p≤0.001, ****p<0.0001
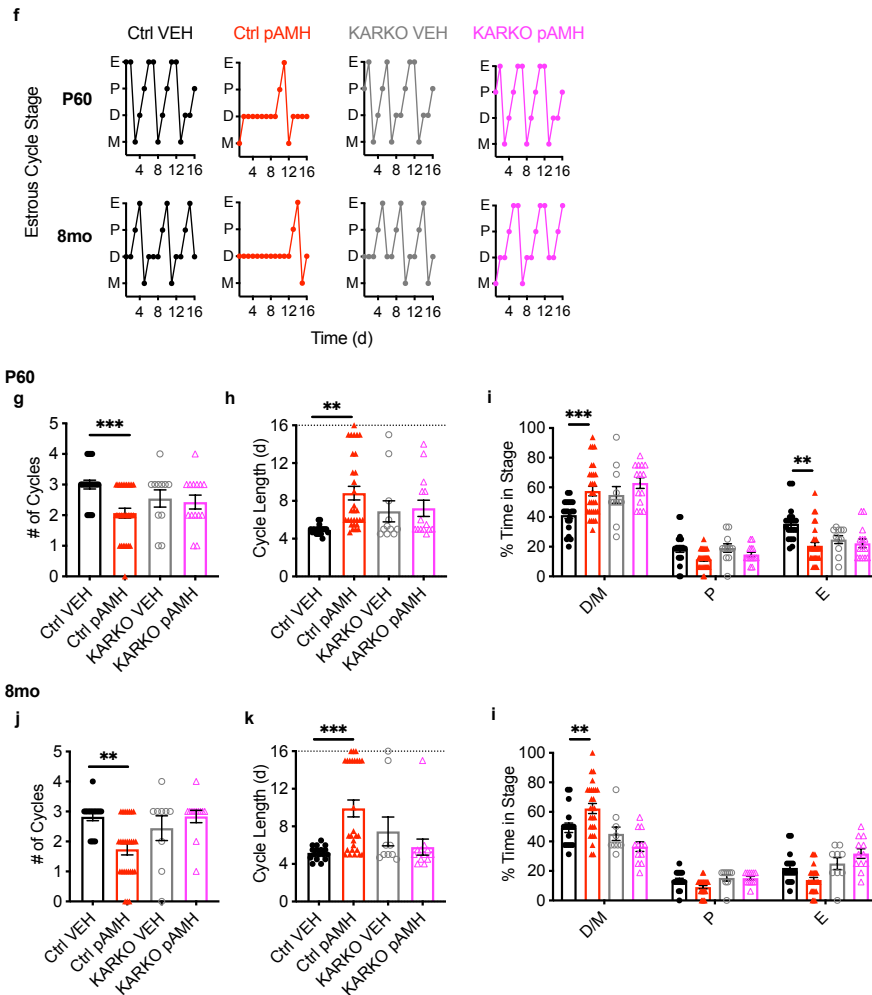
Figure 3.3: pAMH failed to induce reproductive phenotypes in KARKO female offspring, Continued. (f) Representative estrous cycles of the same females of each genotype and treatment at P60 and 8 months of age. E, estrus. P, proestrus. D, diestrus. M, metestrus. In 16-day sampling period for P60 Ctrl (VEH, black, n=20, pAMH, red, n=30) and KARKO (VEH, gray, n=11, pAMH, magenta, n=14) females**, (g)** number of cycles (Number of cycles at P60: Treatment x Genotype, $F_{1,71}$=4.012, p=0.0490; Ctrl p=0.0004, 95% CI of diff [0.3909, 1.476]; KARKO p=0.9246, 95% CI of diff [-0.6402, 0.8740]), **(h)** estrous cycle length (Treatment x Genotype, $F_{1,71}$=5.103, p=0.0270; Ctrl p=0.0001, 95% CI of diff [-6.004, -1.760]; KARKO p=0.9616, 95% CI of diff [-3.261, 2.620]), and **(i)** percent time spent in each estrous cycle stage (Treatment x Genotype x Stage, $F_{2,213}$=2.677, p=0.0431; Ctrl D/M p=0.0003, 95% CI of diff [-27.65, -4.775]; Ctrl P p=0.6732, 95% CI of diff [-4.415, 18.46]; Ctrl E p=0.0017, 95% CI of diff [3.357, 26.23]; KARKO D/M p=0.8803, 95% CI of diff [-24.02, 7.903]; KARKO P p=0.9990, 95% CI of diff [-11.57, 20.36]; KARKO E p>0.9999, 95% CI of diff [-13.51, 18.41]). In the 16-day sampling period in 8-month-old Ctrl (VEH n=17, pAMH n=27) and KARKO (VEH n=9, pAMH n=12) females**, (i)** number of cycles (Treatment x Genotype, $F_{1,61}$=5.563, p=0.0216; Ctrl p=0.0017, 95% CI of diff [0.3329, 1.597]; KARKO p=0.8929, 95% CI of diff [-1.067, 0.7337]) and **(j)** estrous cycle length (Treatment x Genotype, $F_{1,61}$=10.25, p=0.0022; Ctrl p=0.0002, 95% CI of diff [-7.352, -2.090]; KARKO p=0.5246, 95% CI of diff [-2.076, 5.418]). Dotted lines in **(h, k)** indicates the 16-day cut-off. Data were analyzed using **(g-h, j-k)** Two-way ANOVA with Sidak's multiple comparisons test or **(i, l)** Three-way ANOVA with Tukey's multiple comparisons test. **p<0.01, ***p<0.001.
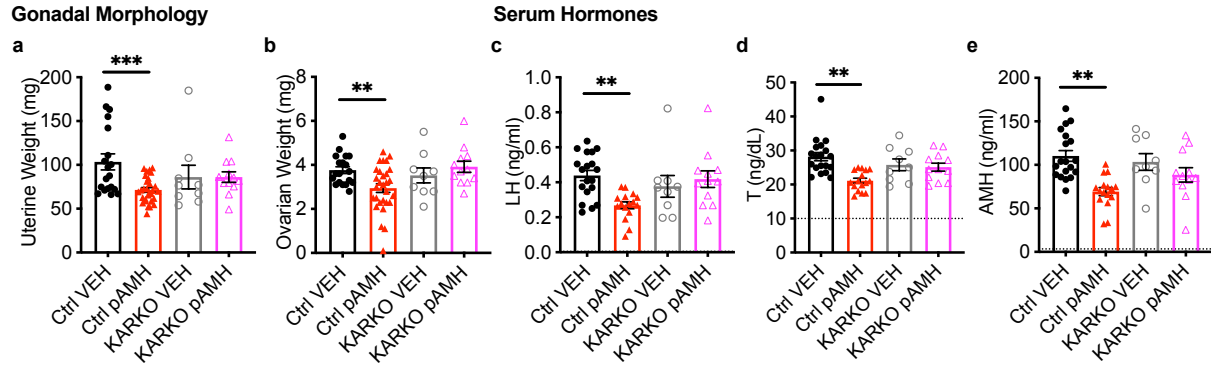
Figure 3.4: KARKO female offspring did not show pAMH-induced alterations in gross gonadal morphology and serum hormones in late adulthood. (a) Uterine and **(b)** ovarian weight of Ctrl (VEH n=19, pAMH n=29) and KARKO (VEH n=9, pAMH n=12) females at 10 months of age. Serum levels of **(c)** LH, **(d)** testosterone (T), and **(e)** AMH in 10-month-old Ctrl (VEH n=19, pAMH n=19) and KARKO (VEH n=9, pAMH n=12) females. Dotted lines in **(d-e)** indicate sensitivity threshold of the hormone assay. Data were analyzed using Two-way ANOVA with Sidak's multiple comparisons test. $**p<0.01$, $***p<0.001$. Uterine weight: Treatment x Genotype, $F_{1,65}=4.566$, $p=0.0364$; Ctrl $p=0.0006$, 95% CI of diff [12.95, 51.16]; KARKO $p>0.9999$, 95% CI of diff [-28.54, 28.54]. Ovarian weight: Treatment x Genotype, $F_{1,65}=6.071$, $p=0.0164$; Ctrl $p=0.0079$, 95% CI of diff [0.1916, 1.445]; KARKO $p=0.5624$, 95% CI of diff [-1.331, 0.5419]. LH: Treatment x Genotype, $F_{1,52}=7.828$, $p=0.0072$; Ctrl $p=0.0010$, 95% CI of diff [0.06461, 0.2771]; KARKO $p=0.7491$, 95% CI of diff [-0.1789, 0.09727]. T: Treatment x Genotype, $F_{1,52}=6.577$, $p=0.0133$; Ctrl $p<0.0001$, 95% CI of diff [3.572, 10.56]; KARKO $p=0.9265$, 95% CI of diff [-3.851, 5.225]. AMH: Treatment x Genotype, $F_{1,52}=4.082$, $p=0.0485$; Ctrl $p<0.0001$, 95% CI of diff [22.90, 59.61]; KARKO $p=0.2907$, 95% CI of diff [-9.009, 38.70].
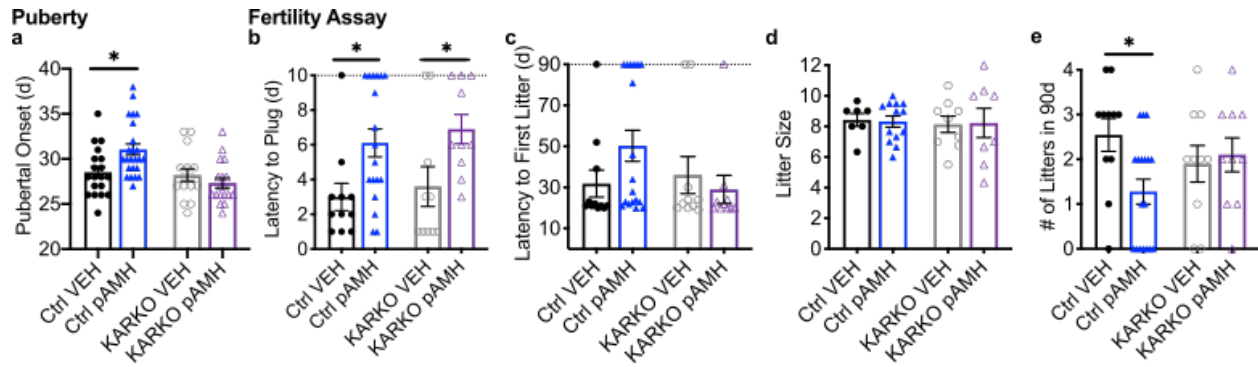
Figure 3.5: pAMH failed to induce most reproductive phenotypes in KARKO male offspring. (a) Pubertal onset measured by preputial separation in Ctrl (VEH, black, n=19, pAMH, blue, n=24) and KARKO (VEH, gray, n=15, pAMH, purple, n=18) males. In a 90-day fertility assay beginning at 3 months of age, Ctrl (VEH n=7, pAMH n=16) and KARKO (VEH n=7, pAMH n=16) males were assessed for **(b)** time to plug by a 10-day cut-off indicated by the dotted line, **(c)** latency to first litter by the 90-day cut-off indicated by the dotted line, **(d)** average litter size per male, and **(e)** total number of litters. Data were analyzed using Two-way ANOVA with Sidak's multiple comparisons test. *p<0.05. Pubertal onset: Treatment x Genotype, $F_{1,72}$=7.016, p=0.0099; Ctrl p=0.0077, 95% CI of diff [-4.440, -0.5908]; KARKO p=0.6022, 95% CI of diff [-1.324, 3.058]. Plugging: Treatment x Genotype, $F_{1,45}$=0.01037, p=0.9197. Treatment, $F_{1,45}$=11.94, p=0.0012; Ctrl p=0.0263, 95% CI of diff -5.902, -0.3204]; KARKO p=0.0469, 95% CI of diff [-6.561, -0.03885]. First Litter: Treatment x Genotype, $F_{1,45}$=2.477, p=0.1225; Treatment, $F_{1,45}$=0.5019, p=0.4823. Litter size: Treatment x Genotype, $F_{1,33}$=0.02845, p=0.8671; Treatment, $F_{1,33}$=0.0002286, p=0.9880. Number of litters: Treatment x Genotype, $F_{1,45}$=4.230, p=0.0455; Ctrl p=0.0178, 95% CI of diff [0.1943, 2.341]; KARKO p=0.9182, 95% CI of diff [-1.454, 1.054].
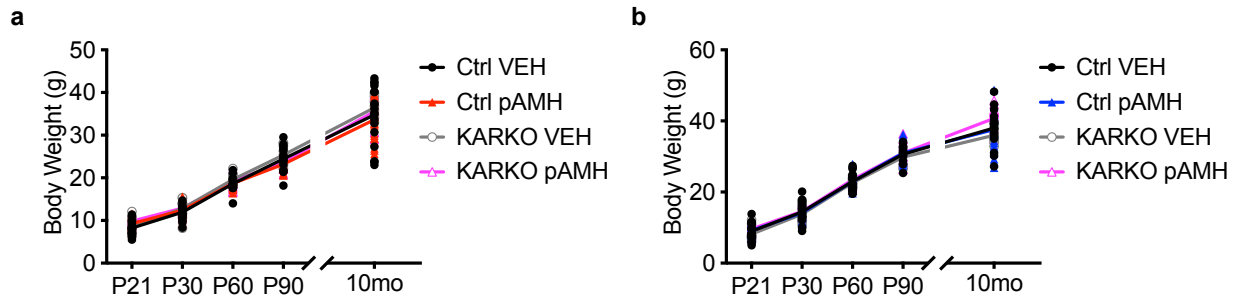
Figure 3.6: pAMH did not significantly affect body weight across the lifespan of KARKO offspring. **(a)** KARKO and Ctrl F_1 females (Treatment x Age, $F_{12,250}$= 1.537, p=0.1113), and **(b)** KARKO and Ctrl F_1 males (Treatment x Age, $F_{12,244}$= 1.656, p=0.1130). Data were analyzed using Mixed-effects model with the Geisser-Greenhouse correction to account for differing variability of differences.

Tables

Table 3.1: Summary of significant transgenerational pAMH phenotypes in female control and KARKO mice. *indicates phenotype is consistent with previous reports (25, 43). Grey shading indicates phenotype was not assayed at that timepoint.

Age	Phenotype		F_1 Generation	F_1 Generation KARKO	F_2 Generation
Peripubertal & Early Adulthood (P30-P60)	Anogenital distance		↑*	ns	↑*
	Pubertal onset	Vaginal opening	↑*	ns	↑*
		First estrus	↑*	ns	↑*
	Serum hormones	LH			↑
		FSH			↓
	Estrous cycling	Time in D/M	↑*	ns	↑*
		# Cycles	↓*	ns	↓*
		Cycle length	↑	ns	↑
Adulthood (3-5mo)	Fertility - # Litters		↓*	ns	↓*
	Uterine weight		↓		ns
	Ovarian changes	Weight	↓		↓
		# CLs	↓*		↓*
		# Late antral follicles	↓*		↓
		Cyp19a1 mRNA	↓		ns
	Serum hormones	LH	↑		↑*
		FSH	↓		↓
		E2	↓		ns
		T	↑		↑*
		AMH	↑		↑
Late Adulthood (8-10mo)	Estrous cycling	Time in D/M	↑	ns	↑
		# Cycles	↓	ns	↓
		Cycle length	↑	ns	↑
	Uterine weight		↓	ns	ns
	Serum hormones	LH	↑	ns	↑
		T	↑	ns	↑
		AMH	↑	ns	↑

Table 3.2: Summary of significant transgenerational pAMH phenotypes in male control and KARKO mice. Grey shading indicates phenotype was not assayed at that timepoint.

Age	Phenotype		F_1 Generation	F_1 Generation KARKO	F_2 Generation
Peripubertal & Early Adulthood (P30-P60)	Pubertal onset		↑	ns	↑
	Serum hormones	LH			ns
		FSH			↓
Adulthood (3-5mo)	Fertility	Latency to plug	↑	↑	ns
		# Litters	↓	ns	
	Serum hormones	LH	ns		
		FSH	↓		↓
		T	ns		

DISCUSSION

Here we demonstrate that androgen receptor (AR) in kisspeptin cells is necessary for the reproductive deficits generated upon prenatal anti-Mullerian hormone (pAMH) exposure in both sexes and expand upon initial reports of deficits in young female mice following pAMH. We show that female offspring of AMH-exposed mice show significant alterations that extend beyond peripubertal and early adult timepoints, well into late adulthood (*Table 3.1*). The majority of these phenotypes are also present in second generation offspring. Notably, we are the first to report that male pAMH offspring also show reproductive deficits, including delayed puberty, decreased fertility, and decreased FSH levels (*Table 3.2*). Further, we have elucidated an underlying mechanism of pAMH-induced effects by demonstrating that AR in kisspeptin cells is necessary for all of the pAMH-induced phenotypes assayed in females and all but one of the pAMH-induced phenotypes assayed in males (*Table 3.1, 3.2*).

By examining female offspring at various ages, the broad scope that pAMH can have across the lifespan becomes evident. Following robust pubertal delays, there is a window of normal reproduction around 3 months of age when pAMH females have normal estrous cycles and fecundity. This window is brief however, and at 5 months, pAMH females have a significant drop-off in fertility, disrupted ovulation, and decreased uterine and ovarian weights compared to vehicle-treated mice. Decreased uterine and ovarian weights continue until 10 months of age, when significant decreases are found in serum LH, testosterone, and AMH levels. Decreased ovarian size, androgen secretion, and AMH levels are all markers of menopause and ovarian failure in women (58). Interestingly, estrous cycling in late adulthood revealed disruptions in pAMH mice distinct from the signs of early reproductive senescence observed following prenatal androgen exposure (44). Reproductive aging in women with PCOS is complex, as the expected

42

follicle loss over time usually correlates with relative normalization of elevated hormone levels and improved regularity of menstrual cycles (58). By these measures, PCOS women have been reported to have a slight increase in reproductive lifespan (59). Although additional research in both clinical settings and mouse models is warranted to understand the relationship between pAMH and reproductive aging, it is clear from our present data that AMH exposure *in utero* is sufficient to have lasting effects in offspring.

We also identified alterations in male offspring. Sons of PCOS women have abnormal FSH, AMH, and androgen levels during the pre- and peripubertal period (12, 13). In ovine models, prenatal androgenization has been found to alter development and function of testicular Leydig cells (55). pAMH male mice showed significant pubertal delays and decreased number of litters in our experiments, which could potentially be explained by decreased FSH. Loss of function mutations in FSH and its receptor have been shown to cause pubertal delays and infertility (60). Although FSH is also known to regulate testicular volume, Sertoli cell number, and transcriptional activation of *Amh* (61), we did not observe any decrease in testicular weight or litter size. AMH levels in adult males were below assay detection level, but LH and testosterone levels in pAMH males were normal. Our findings are similar to those found in mice exposed to prenatal androgens, in which male offspring have normal LH pulses, testosterone, and daily sperm production (62).

We are the first to report that adult AMH levels are increased in pAMH female offspring. AMH has been shown to increase excitability of gonadotropin-releasing hormone (GnRH) neurons in slice preparations of the hypothalamus and stimulate GnRH release from explants of the median eminence (63). AMH can also increase pituitary luteinizing hormone (LH) release *in vivo* (63). Our findings are consistent with human studies that show daughters of PCOS women

have high AMH during infancy, childhood, adolescence, and adulthood (11, 57, 64-66). Because F_1 pAMH female offspring exhibit elevated AMH and androgens during reproductive ages, we sought to identify phenotypes that might carry forward into the next generation. As expected, F_2 female and male offspring generated from pAMH females paired with control males exhibited reproductive deficits to a similar degree as their F_1 generation counterparts (***Table 3.1, 3.2***). Second and third generation pAMH females were recently generated by pairing pAMH females with pAMH males, although it has not been tested whether the pAMH phenotype can be transmitted through the male lineage. Transgenerational transmission of pAMH phenotypes in females were found to occur through hypomethylation and transcriptome changes in DNA isolated from ovaries (43). Of note, while prenatal administration of androgens in mice affects first generation female offspring, reproductive phenotypes do not persist into second and third generations (11). This distinction highlights unique consequences of the pAMH exposure paradigm, and perhaps modulation of AMH levels in pregnancy could ameliorate risk to future offspring. Additional studies are required to distinguish between whether epigenetic changes in later generations are caused by an initial insult to the first generation, or rather perpetuated by disrupted maternal AMH and/or androgens.

In females, pAMH altered both testosterone and AMH levels, with significant increases in adulthood and significant decreases by 10 months of age. A similar relationship between androgens and AMH in females has been previously reported. Androgen supplementation can increase AMH levels (67). AMH decreases ovarian aromatase expression and activity in *in vitro* human (68, 69) and rodent (70) experiments, consistent with a build-up of androgens. Also, administration of AMH during gestation increases maternal testosterone (25). To our knowledge, AMH levels have not been reported in any other mouse model of PCOS that recapitulates

androgen excess. Elevated AMH following prenatal androgen exposure, peripubertal androgen exposure, and/or peripubertal aromatase inhibition would further support a dual mechanism between these hormones. Further investigation of the intersection between androgens and AMH in both clinical and preclinical contexts may provide useful insight into PCOS etiology. Because current AMH and testosterone assays require terminal serum samples, the present experiments were limited in the number of time points we could measure. Future studies with serial hormone sampling may increase the temporal resolution and enable a closer correlation between AMH and/or androgens and reproductive status. For example, perhaps hormone levels are within the range of normal around 3 months of age, and it is only after these levels have the opportunity to build up that estrous cycling and fertility is disrupted. If this were the case, it would further support the clinical utility of interventions normalizing AMH and/or androgen levels.

To test the necessity of androgen signaling at the level of kisspeptin cells, we generated a kisspeptin cell-specific androgen receptor knockout (KARKO) mouse line using Cre-LoxP transgenic mice. Global knockout of AR in female mice delays first estrus, disrupts adult ovulation, decreases fertility, and alters uterine morphology (71, 72). These females also have elevated LH that is unresponsive to negative hormonal feedback, as well as high androgen levels (73). Global AR knockout in males results in an even greater reproductive deficits, with severely altered reproductive tract development and complete infertility (71). Hypothalamic kisspeptin neurons are known regulators of puberty and normal reproductive function, with kisspeptin neurons in the anteroventral periventricular nucleus (AVPV) important for estrogen positive feedback during the preovulatory LH surge and kisspeptin neurons in the arcuate nucleus (ARC) important for negative feedback regulation of LH pulses (74). Therefore, we expected that deleting AR in kisspeptin cells might result in reproductive disruptions. Interestingly, comparing

KARKO and littermate controls (Ctrl) in the vehicle treatment group, we found that deletion of

AR from kisspeptin cells had no effect on any reproductive measure in either sex. This does not

eliminate the possibility that kisspeptin AR regulates reproductive physiology, as there are

potentially redundant pathways such that KARKO alone is insufficient to cause significant

deficits.

The loss of AR in kisspeptin cells is sufficient, however, to prevent the development of

reproductive phenotypes following prenatal AMH exposure. These findings have demonstrated

that pAMH action is mediated by androgenic signaling specifically at the level of kisspeptin cells

in the offspring, allowing us to expand upon the pathophysiological mechanism previously

introduced (25) (*Schema 1*). Elevated AMH binds AMHR2 expressed on maternal GnRH

neurons and placental cells to create an androgenic *in utero* environment for developing

embryos. Because significant pAMH-induced effects were replicated in offspring in the KARKO

study in which the AMH-injected pregnant dams are $AR^{flox/flox}$;$Kisspeptin^{Cre+}$ themselves, and

thus lack AR in their kisspeptin cells during these pregnancies, AR in kisspeptin cells of the

AMH-injected pregnant dams is not needed to induce the phenotype in the pAMH offspring. In

pAMH offspring, hypothalamic signaling to the pituitary likely results in decreased FSH

secretion in both sexes. In females, there is also increased LH secretion. The altered

gonadotropin signal to the ovary decreases aromatase expression and favors increased androgen

and AMH production. Androgens then signal back to the hypothalamus to perpetuate HPG axis

dysregulation and cause reproductive deficits. GnRH neurons themselves do not express AR, so

androgens must modulate the HPG axis at the level of an upstream neuronal population. While

GABAergic neurons have been proposed as potential conduits of reproductive disruptions

following pAMH exposure (25), here we identify kisspeptin cells as necessary for the development of this phenotype.

It remains unclear exactly how androgens are affecting kisspeptin neurons following pAMH exposure. In normal reproduction, androgens exert negative feedback on the HPG axis. From our immunohistochemistry studies, we determined that about half kisspeptin neurons in the ARC express AR, consistent with previous reports in rats (81). Prolonged androgen exposure administered beginning at puberty has been shown to decrease the number of kisspeptin-expressing cells in the ARC, as well as suppress kisspeptin production in these neurons and decrease LH secretion (22). Although we did not directly measure androgen levels at puberty, a previous study found that testosterone was elevated in pAMH mice at 2-hr postnatally and at P60 (25), and we found that LH was elevated in our F_2 pAMH females. It would be therefore be consistent with our understanding of androgen regulation of the HPG axis to propose that elevated androgens suppress the initiation of puberty. However, we saw a robust delay in pubertal onset in both females and males, who did not show significant elevations of testosterone or LH levels above baseline. We speculate that *in utero* androgen exposure in developing embryos are causing an organizational change to the ARC kisspeptin neuronal population in both sexes that alters the initiation of puberty. Although it is difficult to know without more thorough elucidation of the mechanisms driving pubertal onset, these changes may entail modulated hormone receptor expression, ion channel expression, or chromatin remodeling. Parsing out precise mechanisms is further complicated by the seemingly contradictory finding in our adult pAMH females, as well as in PCOS and PCOS-like animal models, that androgen excess seems to exert a stimulatory, positive feedback loop on the HPG axis. Perhaps, after a prolonged inhibitory signal, a threshold is reached and ARC kisspeptin neurons undergo a compensatory

cellular process. There could alternatively be other kisspeptin neuronal populations outside of the hypothalamus that become recruited into the fray once a certain threshold of androgen exposure is reached. Future studies are required to understand how the switch from inhibitory to stimulatory effects of androgens occurs in both clinically and in preclinical models.

Kisspeptin expression in the ARC begins at E13 (78), prior to the first AMH injections, and because the production of kisspeptin drives Cre-induced recombination, kisspeptin AR in the KARKO mouse is deleted from offspring *in utero* as well as in adulthood. As such, the present experiments are unable to distinguish mechanistically between prenatal programming effects and continual maintenance of the phenotype by elevated androgens. In both female and male mice, neural circuits between ARC kisspeptin neurons and GnRH neurons are established before birth (78, 79). Androgen exposure *in utero* has been shown to have lasting organizational effects (44), whereas peripubertal androgen excess results in transient reproductive deficits (44, 80). Novel experimental tools, such the development of an inducible Kisspeptin-Cre, would enable investigation into the timing of androgenic mechanisms.

We have determined the necessity of AR in kisspeptin cells for pAMH-induced phenotypes, but the question of which kisspeptin cell population remains. AR is expressed in the majority of ARC kisspeptin neurons but only in less than 2% of AVPV kisspeptin neurons in females (81), and concordantly, androgens directly suppress ARC, but not AVPV, kisspeptin neurons (22). The present KARKO experiments do not eliminate the possibility of AR action in the gonads, as kisspeptin is expressed in both the ovaries and testes (82, 83). In the rodent ovary, there appears to be limited overlap between kisspeptin- and AR-expressing cells. AR is expressed in theca cells (84) and granulosa cells of follicles from the primordial to secondary developmental stage (85), while kisspeptin expression has been reported in the interstitial, theca,

and granulosa cells of preovulatory follicles (86). Although there is a potential for a population of theca cells with overlap of AR and kisspeptin, studies utilizing a theca cell-specific knockout of AR indicate that AR does not influence fertility or androgen levels in female mice (87). The significant changes in gonadotropin levels and the reversal of phenotypes in both sexes, also point toward a mechanism upstream of the gonads. A central mechanism is further suggested by the abundance of evidence speaking to the critical role hypothalamic kisspeptin neurons play in reproduction (74) and the fact that GnRH antagonism in pAMH offspring is sufficient to reverse reproductive phenotypes (25). The significant changes in gonadotropin levels also point toward a mechanism upstream of the gonads. Future studies, perhaps utilizing gonadectomy, may further clarify the tissue specific kisspeptin cell populations in which androgens are acting to mediate pAMH phenotypes.

pAMH induced reproductive changes in control (Ctrl) but not KARKO mice across the board, suggesting a common underlying androgenic mechanism mediating all changes. The single exception to this pattern was in the male plugging assay, in which pAMH delayed copulatory behavior in both Ctrl and KARKO, suggesting that the effect may be driven by a mechanism distinct from that mediating all other phenotypes assayed. A male's propensity to plug is driven by several factors (75), including anxiety levels which have been shown to modulate sexual behaviors (76). Prenatal androgen exposure is known to increase anxiety measures in male offspring (77), however, the effects of pAMH on behavioral measures has yet to be explored. If pAMH males have increased anxiety levels, this could explain the delayed plugging via a mechanism independent of kisspeptin AR.

Taken together, our work advances understanding of the consequences of prenatal AMH exposure and highlights androgen signaling in kisspeptin cells as a crucial piece of the

underlying mechanism. These results could have great implications for clinical populations in which AMH and/or androgens are elevated during pregnancy, including common disorders like PCOS. The long-lasting effects of prenatal AMH exposure on offspring highlights a potential need for screening and closer monitoring of gestational AMH. Mothers with elevated AMH may need to be counseled on the potential consequences to their children, including reproductive delays and fertility challenges in adulthood. Couples trying to conceive should both be questioned for maternal history of PCOS or elevated gestational AMH, and it may be appropriate for such individuals to have a lower threshold for referrals to reproductive endocrinology and infertility specialists.

Our findings also suggest that modulation of AMH could have therapeutic value. Although there are currently no pharmacological antagonists for AMHR2, there are known antagonists targeting components of AMHR2 signaling cascade, including all AMH type-I receptors, ALK2/ACVR1, ALK3/BMPR1A, and ALK6/BMPR1B (88). Additionally, given the interaction between AMH and androgens, there may certainly be a role for anti-androgenic treatments, of which there exist several options currently used to treat fertility deficits in PCOS patients (6). AMH modulation also has the potential to help female offspring in adulthood, perhaps by decreasing the accumulation of immature follicles and aiding in the release of single, dominant follicle for ovulation (89). However, the use of such hormone blockers during pregnancy is generally contraindicated due to the iatrogenic risks conferred to the fetus, so they may not be appropriate in trying to prevent initial *in utero* programming. Further elucidation of the cellular and molecular mechanisms mediating pAMH effects may lead to novel preventative interventions and treatment options for PCOS patients and their children.

Schemas
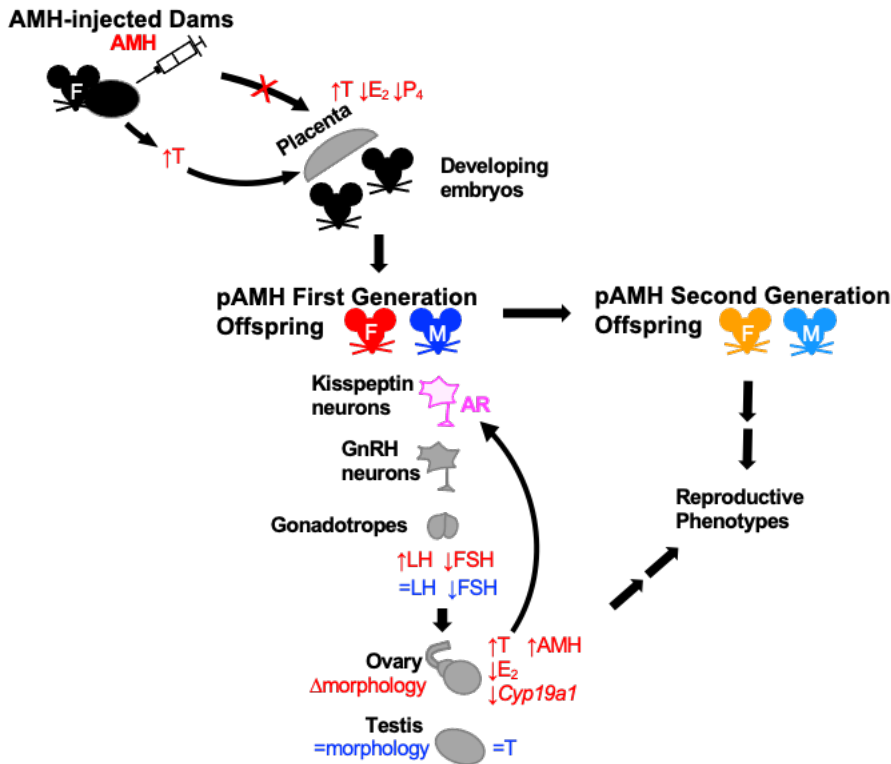
Schema 1: Proposed mechanism of prenatal AMH-induced reproductive phenotypes in mice.
Peripherally-injected AMH in pregnant dams does not cross the placenta but rather affects maternal hypothalamic neurons and placental gene expression to create an androgenic *in utero* environment for developing embryos (25). In pAMH female offspring, hyperexcitable GnRH neurons signal to pituitary gonadotropes to increase LH and decrease FSH. The altered gonadotropin signal to the ovary decreases aromatase (*Cyp19a1)* expression and favors increased androgen and AMH production over estrogen. Androgens then signal back to kisspeptin neurons in the arcuate nucleus of the hypothalamus to perpetuate reproductive neuroendocrine dysregulation. This androgen signal causes reproductive deficits. In male offspring, pAMH-induces decreased FSH through an androgen-mediated mechanism at the level of kisspeptin neurons that results in reproductive deficits. Second generation offspring from pAMH females also exhibit significant deficits, likely through a similar centralized mechanism. Testosterone, T. Estradiol, E_2. Progesterone, P_4.

REFERENCES

1. Sirmans, S. M., and Pate, K. A. (2013) Epidemiology, diagnosis, and management of polycystic ovary syndrome. *Clin Epidemiol* **6**, 1-13

2. Forslund, M., Schmidt, J., Brannstrom, M., Landin-Wilhelmsen, K., and Dahlgren, E. (2021) Reproductive hormones and anthropometry: a follow-up of PCOS and controls from perimenopause to older than 80 years. *J Clin Endocrinol Metab* **106**, 421-430

3. Rosenfield, R. L., Barnes, R. B., Cara, J. F., and Lucky, A. W. (1990) Dysregulation of cytochrome P450c17α as the cause of polycystic ovarian syndrome. *Fertil Steril* **53**, 785-791

4. Peng, C. Y., Xie, H. J., Guo, Z. F., Nie, Y. L., Chen, J., Zhou, J. M., and Yin, J. (2014) The association between androgen receptor gene CAG polymorphism and polycystic ovary syndrome: a case-control study and meta-analysis. *J Assist Reprod Genet* **31**, 1211-1219

5. Sharma, P., Kaur, M., and Khetarpal, P. (2020) CYP19 gene rs2414096 variant and differential genetic risk of polycystic ovary syndrome: a systematic review and meta-analysis. *Gynecol Endocrinol* **37**, 1-6

6. Bachelot, A., Chabbert-Buffet, N., Salenave, S., Kerlan, V., and Galand-Portier, M. B. (2010) Anti-androgen treatments. *Ann Endocrinol (Paris)* **71**, 19-24

7. Sir-Petermann, T., Maliqueo, M., Angel, B., Lara, H. E., Perez-Bravo, F., and Recabarren, S. E. (2002) Maternal serum androgens in pregnant women with polycystic ovarian syndrome: possible implications in prenatal androgenization. *Hum Reprod* **17**, 2573-2579

8. Barry, J. A., Kay, A. R., Navaratnarajah, R., Iqbal, S., Bamfo, J. E., David, A. L., Hines, M., and Hardiman, P. J. (2010) Umbilical vein testosterone in female infants born to mothers with polycystic ovary syndrome is elevated to male levels. *J Obstet Gynaecol* **30**, 444-446

9. Anderson, H., Fogel, N., Grebe, S. K., Singh, R. J., Taylor, R. L., and Dunaif, A. (2010) Infants of women with polycystic ovary syndrome have lower cord blood androstenedione and estradiol levels. *J Clin Endocrinol Metab* **95**, 2180-2186

10.	Maliqueo, M., Lara, H. E., Sanchez, F., Echiburu, B., Crisosto, N., and Sir-Petermann, T. (2013) Placental steroidogenesis in pregnant women with polycystic ovary syndrome. *Eur J Obstet Gynecol Reprod Biol* **166**, 151-155

11.	Risal, S., Pei, Y., Lu, H., Manti, M., Fornes, R., Pui, H. P., Zhao, Z., Massart, J., Ohlsson, C., Lindgren, E., Crisosto, N., Maliqueo, M., Echiburu, B., Ladron de Guevara, A., Sir-Petermann, T., Larsson, H., Rosenqvist, M. A., Cesta, C. E., Benrick, A., Deng, Q., and Stener-Victorin, E. (2019) Prenatal androgen exposure and transgenerational susceptibility to polycystic ovary syndrome. *Nat Med* **25**, 1894-1904

12.	Crisosto, N., Echiburu, B., Maliqueo, M., Luchsinger, M., Rojas, P., Recabarren, S., and Sir-Petermann, T. (2017) Reproductive and metabolic features during puberty in sons of women with polycystic ovary syndrome. *Endocr Connect* **6**, 607-613

13.	Recabarren, S. E., Sir-Petermann, T., Rios, R., Maliqueo, M., Echiburu, B., Smith, R., Rojas-Garcia, P., Recabarren, M., and Rey, R. A. (2008) Pituitary and testicular function in sons of women with polycystic ovary syndrome from infancy to adulthood. *J Clin Endocrinol Metab* **93**, 3318-3324

14.	Azziz, R., Carmina, E., Chen, Z., Dunaif, A., Laven, J. S., Legro, R. S., Lizneva, D., Natterson-Horowtiz, B., Teede, H. J., and Yildiz, B. O. (2016) Polycystic ovary syndrome. *Nat Rev Dis Primers* **2**, 16057

15.	Vink, J. M., Sadrzadeh, S., Lambalk, C. B., and Boomsma, D. I. (2006) Heritability of polycystic ovary syndrome in a Dutch twin-family study. *J Clin Endocrinol Metab* **91**, 2100-2104

16.	Walters, K. A., Edwards, M. C., Tesic, D., Caldwell, A. S. L., Jimenez, M., Smith, J. T., and Handelsman, D. J. (2018) The role of central androgen receptor actions in regulating the hypothalamic-pituitary-ovarian axis. *Neuroendocrinology* **106**, 389-400

17.	Waldstreicher, J., Santoro, N. F., Hall, J. E., Filicori, M., and Crowley, W. F., Jr. (1988) Hyperfunction of the hypothalamic-pituitary axis in women with polycystic ovarian disease: indirect evidence for partial gonadotroph desensitization. *J Clin Endocrinol Metab* **66**, 165-172

18.	Reed, B. G., and Carr, B. R. (2018) The normal menstrual cycle and the control of ovulation. In: Feingold, K. R., Anawalt, B., and Boyce, A., editors. *Endotext* [Internet]. South Dartmouth (MA): MDText.com, Inc.; 2000-. Available from: https://www.ncbi.nlm.nih.gov/books/NBK279054/

19.   Oduwole, O. O., Peltoketo, H., and Huhtaniemi, I. T. (2018) Role of Follicle-Stimulating Hormone in Spermatogenesis. *Front Endocrinol* **9**, 763

20.   Tng, E. L. (2015) Kisspeptin signalling and its roles in humans. *Singapore Med J* **56**, 649-656

21.   Tena-Sempere, M. (2010) Kisspeptin/GPR54 system as potential target for endocrine disruption of reproductive development and function. *Intl J Androl* **33**, 360-368

22.   Iwata, K., Kunimura, Y., and Ozawa, H. (2019) Hypothalamic Kisspeptin Expression in Hyperandrogenic Female Rats and Aging Rats. *Acta Histochem Cytochem* **52**, 85-91

23.   Coyle, C., and Campbell, R. E. (2019) Pathological pulses in PCOS. *Mol Cell Endocrinol* **498**, 110561

24.   Esparza, L. A., Schafer, D., Ho, B. S., Thackray, V. G., and Kauffman, A. S. (2020) Hyperactive LH pulses and elevated kisspeptin and NKB gene expression in the arcuate nucleus of a PCOS mouse model. *Endocrinology* **161**, bqaa018

25.   Tata, B., Mimouni, N. E. H., Barbotin, A. L., Malone, S. A., Loyens, A., Pigny, P., Dewailly, D., Catteau-Jonard, S., Sundstrom-Poromaa, I., Piltonen, T. T., Dal Bello, F., Medana, C., Prevot, V., Clasadonte, J., and Giacobini, P. (2018) Elevated prenatal anti-Mullerian hormone reprograms the fetus and induces polycystic ovary syndrome in adulthood. *Nat Med* **24**, 834-846

26.   Witchel, S. F., and Tena-Sempere, M. (2013) The Kiss1 system and polycystic ovary syndrome: lessons from physiology and putative pathophysiologic implications. *Fertil Steril* **100**, 12-22

27.   McLennan, I. S., and Pankhurst, M. W. (2015) Anti-Mullerian hormone is a gonadal cytokine with two circulating forms and cryptic actions. *J Endocrinol* **226**, R45-57

28.   Garg, D., and Tal, R. (2016) The role of AMH in the pathophysiology of polycystic ovarian syndrome. *Reprod Biomed Online* **33**, 15-28

29.   Abbara, A., Eng, P. C., Phylactou, M., Clarke, S. A., Hunjan, T., Roberts, R., Vimalesvaran, S., Christopoulos, G., Islam, R., Purugganan, K., Comninos, A. N., Trew, G. H., Salim, R., Hramyka, A., Owens, L., Kelsey, T., and Dhillo, W. S. (2019) Anti-

Mullerian hormone (AMH) in the diagnosis of menstrual disturbance due to polycystic ovarian syndrome. *Front Endocrinol (Lausanne)* **10**, 656

30.   Eldar-Geva, T., Margalioth, E. J., Gal, M., Ben-Chetrit, A., Algur, N., Zylber-Haran, E., Brooks, B., Huerta, M., and Spitz, I. M. (2005) Serum anti-Mullerian hormone levels during controlled ovarian hyperstimulation in women with polycystic ovaries with and without hyperandrogenism. *Hum Reprod* **20**, 1814-1819

31.   Lin, Y. H., Chiu, W. C., Wu, C. H., Tzeng, C. R., Hsu, C. S., and Hsu, M. I. (2011) Antimullerian hormone and polycystic ovary syndrome. *Fertil Steril* **96**, 230-235

32.   Piouka, A., Farmakiotis, D., Katsikis, I., Macut, D., Gerou, S., and Panidis, D. (2009) Anti-Mullerian hormone levels reflect severity of PCOS but are negatively influenced by obesity: relationship with increased luteinizing hormone levels. *Am J Physiol Endocrinol Metab* **296**, E238-243

33.   Pigny, P., Merlen, E., Robert, Y., Cortet-Rudelli, C., Decanter, C., Jonard, S., and Dewailly, D. (2003) Elevated serum level of anti-mullerian hormone in patients with polycystic ovary syndrome: relationship to the ovarian follicle excess and to the follicular arrest. *J Clin Endocrinol Metab* **88**, 5957-5962

34.   Kevenaar, M. E., Laven, J. S., Fong, S. L., Uitterlinden, A. G., de Jong, F. H., Themmen, A. P., and Visser, J. A. (2008) A functional anti-mullerian hormone gene polymorphism is associated with follicle number and androgen levels in polycystic ovary syndrome patients. *J Clin Endocrinol Metab* **93**, 1310-1316

35.   Gorsic, L. K., Kosova, G., Werstein, B., Sisk, R., Legro, R. S., Hayes, M. G., Teixeira, J. M., Dunaif, A., and Urbanek, M. (2017) Pathogenic anti-Mullerian hormone variants in polycystic ovary syndrome. *J Clin Endocrinol Metab* **102**, 2862-2872

36.   Gorsic, L. K., Dapas, M., Legro, R. S., Hayes, M. G., and Urbanek, M. (2019) Functional genetic variation in the anti-Mullerian hormone pathway in women with polycystic ovary syndrome. *J Clin Endocrinol Metab* **104**, 2855-2874

37.   Nardo, L. G., Yates, A. P., Roberts, S. A., Pemberton, P., and Laing, I. (2009) The relationships between AMH, androgens, insulin resistance and basal ovarian follicular status in non-obese subfertile women with and without polycystic ovary syndrome. *Hum Reprod* **24**, 2917-2923

38.   Pellatt, L., Hanna, L., Brincat, M., Galea, R., Brain, H., Whitehead, S., and Mason, H. (2007) Granulosa cell production of anti-Mullerian hormone is increased in polycystic ovaries. *J Clin Endocrinol Metab* **92**, 240-245

39.   Pigny, P., Jonard, S., Robert, Y., and Dewailly, D. (2006) Serum anti-Mullerian hormone as a surrogate for antral follicle count for definition of the polycystic ovary syndrome. *J Clin Endocrinol Metab* **91**, 941-945

40.   Iliodromiti, S., Kelsey, T. W., Anderson, R. A., and Nelson, S. M. (2013) Can anti-Mullerian hormone predict the diagnosis of polycystic ovary syndrome? A systematic review and meta-analysis of extracted data. *J Clin Endocrinol Metab* **98**, 3332-3340

41.   Das, M., Gillott, D. J., Saridogan, E., and Djahanbakhch, O. (2008) Anti-Mullerian hormone is increased in follicular fluid from unstimulated ovaries in women with polycystic ovary syndrome. *Hum Reprod* **23**, 2122-2126

42.   Piltonen, T. T., Giacobini, P., Edvinsson, A., Hustad, S., Lager, S., Morin-Papunen, L., Tapanainen, J. S., Sundstrom-Poromaa, I., and Arffman, R. K. (2019) Circulating antimullerian hormone and steroid hormone levels remain high in pregnant women with polycystic ovary syndrome at term. *Fertil Steril* **111**, 588-596 e581

43.   Mimouni, N. E. H., Paiva, I., Barbotin, A. L., Timzoura, F. E., Plassard, D., Le Gras, S., Ternier, G., Pigny, P., Catteau-Jonard, S., Simon, V., Prevot, V., Boutillier, A. L., and Giacobini, P. (2021) Polycystic ovary syndrome is transmitted via a transgenerational epigenetic process. *Cell Metab* **33**, 513-530.e8

44.   Witham, E. A., Meadows, J. D., Shojaei, S., Kauffman, A. S., and Mellon, P. L. (2012) Prenatal exposure to low levels of androgen accelerates female puberty onset and reproductive senescence in mice. *Endocrinology* **153**, 4522-4532

45.   Moore, A. M., Prescott, M., and Campbell, R. E. (2013) Estradiol negative and positive feedback in a prenatal androgen-induced mouse model of polycystic ovarian syndrome. *Endocrinology* **154**, 796-806

46.   Roland, A. V., Nunemaker, C. S., Keller, S. R., and Moenter, S. M. (2010) Prenatal androgen exposure programs metabolic dysfunction in female mice. *J Endocrinol* **207**, 213-223

47.   Walters, K. A. (2016) Androgens in polycystic ovary syndrome: lessons from experimental models. *Curr Opin Endocrinol Diabetes Obes* **23**, 257-263

48. Yoo, S. H., Yamazaki, S., Lowrey, P. L., Shimomura, K., Ko, C. H., Buhr, E. D., Siepka, S. M., Hong, H. K., Oh, W. J., Yoo, O. J., Menaker, M., and Takahashi, J. S. (2004) PERIOD2::LUCIFERASE real-time reporting of circadian dynamics reveals persistent circadian oscillations in mouse peripheral tissues. *Proc Natl Acad Sci* **101**, 5339-5346

49. Mereness, A. L., Murphy, Z. C., and Sellix, M. T. (2015) Developmental programming by androgen affects the circadian timing system in female mice. *Biol Reprod* **92**, 88

50. Yeh, S., Tsai, M. Y., Xu, Q., Mu, X. M., Lardy, H., Huang, K. E., Lin, H., Yeh, S. D., Altuwaijri, S., Zhou, X., Xing, L., Boyce, B. F., Hung, M. C., Zhang, S., Gan, L., and Chang, C. (2002) Generation and characterization of androgen receptor knockout (ARKO) mice: an in vivo model for the study of androgen functions in selective tissues. *Proc Natl Acad Sci* **99**, 13498-13503

51. Cravo, R. M., Margatho, L. O., Osborne-Lawrence, S., Donato, J., Jr., Atkin, S., Bookout, A. L., Rovinsky, S., Frazao, R., Lee, C. E., Gautron, L., Zigman, J. M., and Elias, C. F. (2011) Characterization of Kiss1 neurons using transgenic mouse models. *Neuroscience* **173**, 37-56

52. Madisen, L., Zwingman, T. A., Sunkin, S. M., Oh, S. W., Zariwala, H. A., Gu, H., Ng, L. L., Palmiter, R. D., Hawrylycz, M. J., Jones, A. R., Lein, E. S., and Zeng, H. (2010) A robust and high-throughput Cre reporting and characterization system for the whole mouse brain. *Nat Neurosci* **13**, 133-140

53. Cora, M. C., Kooistra, L., and Travlos, G. (2015) Vaginal cytology of the laboratory rat and mouse: review and criteria for the staging of the estrous cycle using stained vaginal smears. *Toxicol Pathol* **43**, 776-793

54. Koebele, S. V., and Bimonte-Nelson, H. A. (2016) Modeling menopause: The utility of rodents in translational behavioral endocrinology research. *Maturitas* **87**, 5-17

55. Connolly, F., Rae, M. T., Bittner, L., Hogg, K., McNeilly, A. S., and Duncan, W. C. (2013) Excess androgens in utero alters fetal testis development. *Endocrinology* **154**, 1921-1933

56. Cannarella, R., Condorelli, R. A., Mongioi, L. M., La Vignera, S., and Calogero, A. E. (2018) Does a male polycystic ovarian syndrome equivalent exist? *J Endocrinol Invest* **41**, 49-57

57. Sir-Petermann, T., Ladron de Guevara, A., Codner, E., Preisler, J., Crisosto, N., Echiburu, B., Maliqueo, M., Sanchez, F., Perez-Bravo, F., and Cassorla, F. (2012) Relationship between anti-Mullerian hormone (AMH) and insulin levels during different tanner stages in daughters of women with polycystic ovary syndrome. *Reprod Sci* **19**, 383-390

58. Hsu, M. I. (2013) Changes in the PCOS phenotype with age. *Steroids* **78**, 761-766

59. Tehrani, F. R., Solaymani-Dodaran, M., Hedayati, M., and Azizi, F. (2010) Is polycystic ovary syndrome an exception for reproductive aging? *Hum Reprod* **25**, 1775-1781

60. Layman LC, M. P. (2000) Mutations of follicle stimulating hormone-β and its receptor in human and mouse: genotype/phenotype. *Mol Cell Endocrinol* **161**, 9-17

61. Xu, H. Y., Zhang, H. X., Xiao, Z., Qiao, J., and Li, R. (2019) Regulation of anti-Mullerian hormone (AMH) in males and the associations of serum AMH with the disorders of male fertility. *Asian J Androl* **21**, 109-114

62. Holland, S., Prescott, M., Pankhurst, M., and Campbell, R. E. (2019) The influence of maternal androgen excess on the male reproductive axis. *Sci Rep* **9**, 18908

63. Cimino, I., Casoni, F., Liu, X., Messina, A., Parkash, J., Jamin, S. P., Catteau-Jonard, S., Collier, F., Baroncini, M., Dewailly, D., Pigny, P., Prescott, M., Campbell, R., Herbison, A. E., Prevot, V., and Giacobini, P. (2016) Novel role for anti-Mullerian hormone in the regulation of GnRH neuron excitability and hormone secretion. *Nat Commun* **7**, 10055

64. Sir-Petermann, T., Codner, E., Maliqueo, M., Echiburu, B., Hitschfeld, C., Crisosto, N., Perez-Bravo, F., Recabarren, S. E., and Cassorla, F. (2006) Increased anti-Mullerian hormone serum concentrations in prepubertal daughters of women with polycystic ovary syndrome. *J Clin Endocrinol Metab* **91**, 3105-3109

65. Crisosto, N., Codner, E., Maliqueo, M., Echiburu, B., Sanchez, F., Cassorla, F., and Sir-Petermann, T. (2007) Anti-Mullerian hormone levels in peripubertal daughters of women with polycystic ovary syndrome. *J Clin Endocrinol Metab* **92**, 2739-2743

66. Olszanecka-Glinianowicz M, Z. A., Drosdzol-Cop A, Bożętowicz-Wikarek M, Owczarek A, Gawlik A, Chudek J, Skrzypulec-Plinta V, Małecka-Tendera E. (2016) Circulating anti-Müllerian hormone levels in daughters of women with and without polycystic ovary syndrome. *Horm Res Paediatr* **85**, 372-378

67.   Fouany, M. R., and Sharara, F. I. (2013) Is there a role for DHEA supplementation in women with diminished ovarian reserve? *J Assist Reprod Genet* **30**, 1239-1244

68.   Grossman, M. P., Nakajima, S. T., Fallat, M. E., and Siow, Y. (2008) Mullerian-inhibiting substance inhibits cytochrome P450 aromatase activity in human granulosa lutein cell culture. *Fertil Steril* **89**, 1364-1370

69.   Chang, H. M., Klausen, C., and Leung, P. C. (2013) Antimullerian hormone inhibits follicle-stimulating hormone-induced adenylyl cyclase activation, aromatase expression, and estradiol production in human granulosa-lutein cells. *Fertil Steril* **100**, 585-592 e581

70.   di Clemente, N., Wilson, C., Faure, E., Boussin, L., Carmillo, P., Tizard, R., Picard, J. Y., Vigier, B., Josso, N., and Cate, R. (1994) Cloning, expression, and alternative splicing of the receptor for anti-Mullerian hormone. *Mol Endocrinol* **8**, 1006-1020

71.   Zhou, X. (2010) Roles of androgen receptor in male and female reproduction: lessons from global and cell-specific androgen receptor knockout (ARKO) mice. *J Androl* **31**, 235-243

72.   Walters KA, M. K., Seneviratne MG, Jimenez M, McMahon AC, Allan CM, Salamonsen LA, Handelsman DJ. (2009) Subfertile female androgen receptor knockout mice exhibit defects in neuroendocrine signaling, intraovarian function, and uterine development but not uterine function. *Endocrinology* **150**, 3274-3282

73.   Cheng, X. B., Jimenez, M., Desai, R., Middleton, L. J., Joseph, S. R., Ning, G., Allan, C. M., Smith, J. T., Handelsman, D. J., and Walters, K. A. (2013) Characterizing the neuroendocrine and ovarian defects of androgen receptor-knockout female mice. *Am J Physiol Endocrinol Metab* **305**, E717-726

74.   Smith, J. (2013) Sex Steroid Regulation of Kisspeptin Circuits. In *Kisspeptin Signaling in Reproductive Biology. Advances in Experimental Medicine and Biology* (Kauffman A., S. J., ed) Vol. 784, Springer, New York, NY

75.   Schneider, M. R., Mangels, R., and Dean, M. D. (2016) The molecular basis and reproductive function(s) of copulatory plugs. *Mol Reprod Dev* **83**, 755-767

76.   Francesca R. D'Amato, F. P. (1992) Role of anxiety in subordinate male mice sexual behavior. *Pharmacol Biochem Behav* **43**, 181-185

77. Risal, S., Manti, M., Lu, H., Fornes, R., Larsson, H., Benrick, A., Deng, Q., Cesta, C. E., Rosenqvist, M. A., and Stener-Victorin, E. (2021) Prenatal androgen exposure causes a sexually dimorphic transgenerational increase in offspring susceptibility to anxiety disorders. *Transl Psychiatry* **11**, 45

78. Kumar, D., Freese, M., Drexler, D., Hermans-Borgmeyer, I., Marquardt, A., and Boehm, U. (2014) Murine arcuate nucleus kisspeptin neurons communicate with GnRH neurons in utero. *J Neurosci* **34**, 3756-3766

79. Kumar, D., Periasamy, V., Freese, M., Voigt, A., and Boehm, U. (2015) In utero development of kisspeptin/GnRH neural circuitry in male mice. *Endocrinology* **156**, 3084-3090

80. Kauffman, A. S., Thackray, V. G., Ryan, G. E., Tolson, K. P., Glidewell-Kenney, C. A., Semaan, S. J., Poling, M. C., Iwata, N., Breen, K. M., Duleba, A. J., Stener-Victorin, E., Shimasaki, S., Webster, N. J., and Mellon, P. L. (2015) A novel letrozole model recapitulates both the reproductive and metabolic phenotypes of polycystic ovary syndrome in female mice. *Biol Reprod* **93**, 69

81. Iwata, K., Kunimura, Y., Matsumoto, K., and Ozawa, H. (2017) Effect of androgen on Kiss1 expression and luteinizing hormone release in female rats. *J Endocrinol* **233**, 281-292

82. Merhi, Z., Thornton, K., Bonney, E., Cipolla, M. J., Charron, M. J., and Buyuk, E. (2016) Ovarian kisspeptin expression is related to age and to monocyte chemoattractant protein-1. *J Assist Reprod Genet* **33**, 535-543

83. Salehi, S., Adeshina, I., Chen, H., Zirkin, B. R., Hussain, M. A., Wondisford, F., Wolfe, A., and Radovick, S. (2015) Developmental and endocrine regulation of kisspeptin expression in mouse Leydig cells. *Endocrinology* **156**, 1514-1522

84. Pelletier, G., Labrie, C., and Labrie, F. (2000) Localization of oestrogen receptor alpha, oestrogen receptor beta and androgen receptors in the rat reproductive organs. *J Endocrinol* **165**, 359-370

85. Yang, R., Yang, S., Li, R., Liu, P., Qiao, J., and Zhang, Y. (2016) Effects of hyperandrogenism on metabolic abnormalities in patients with polycystic ovary syndrome: a meta-analysis. *Reprod Biol Endocrinol* **14**, 1-10

86.   Castellano, J. M., Gaytan, M., Roa, J., Vigo, E., Navarro, V. M., Bellido, C., Dieguez, C., Aguilar, E., Sanchez-Criado, J. E., Pellicer, A., Pinilla, L., Gaytan, F., and Tena-Sempere, M. (2006) Expression of KiSS-1 in rat ovary: putative local regulator of ovulation? *Endocrinology* **147**, 4852-4862

87.   Ma, Y., Andrisse, S., Chen, Y., Childress, S., Xue, P., Wang, Z., Jones, D., Ko, C., Divall, S., and Wu, S. (2017) Androgen receptor in the ovary theca cells plays a critical role in androgen-induced reproductive dysfunction. *Endocrinology* **158**, 98-108

88.   Mohedas, A. H., Xing, X., Armstrong, K. A., Bullock, A. N., Cuny, G. D., and Yu, P. B. (2013) Development of an ALK2-biased BMP type I receptor kinase inhibitor. *ACS Chem Biol* **8**, 1291-1302

89.   Kushnir, V. A., Seifer, D. B., Barad, D. H., Sen, A., and Gleicher, N. (2017) Potential therapeutic applications of human anti-Müllerian hormone (AMH) analogues in reproductive medicine. *J Assist Reprod Genet* **34**, 1105-1113